Direct absorption nanofluid-based solar collectors for low and medium temperatures. A review

Miguel Sainz Mañas, Françoise Bataille, Cyril Caliot, Alexis Vossier, Gilles Flamant

Direct absorption nanofluid-based solar collectors for low and medium temperatures. A review

Miguel Sainz Mañas[1], Françoise Bataille[1], Cyril Caliot[2], Alexis Vossier[1], Gilles Flamant[1]

[1] Processes, Materials and Solar Energy laboratory, PROMES - CNRS, UPVD, 7 rue du Four Solaire, 66120 Font-Romeu Odeillo and rambla de la Thermodynamique, Tecnosud, 66100 Perpignan, France.

[2] Laboratory of Mathematics and its Applications, Université de Pau et des Pays de l'Adour, E2S UPPA, CNRS, LMAP, allée du parc Montaury, 64600 Anglet, France.

ABSTRACT

Solar energy is expected to play an important role in the decarbonization of the energy and industrial sectors. Low and medium temperature (< 400 °C) solar thermal collectors have proved to be a reliable solution to supply heat and decarbonize the industrial sector, with over 800 Solar Heat for Industrial Processes (SHIP) plants put in operation in the last decade. Governmental support policy is a key factor for solar thermal energy to play a major role in CO_2 emission reduction, which require improving the efficiency of solar collectors and reducing costs. Recent studies have demonstrated the potential of nanoparticles to enhance the optical properties of heat transfer fluids for direct absorption solar collectors (DASC). In a DASC the transfer fluid absorbs volumetrically the incident radiation, resulting in a more homogeneous temperature distribution and less heat losses than in conventional surface collectors. In this paper, the current state-of-the-art of SHIP installations and conventional surface collectors is presented, and a critical literature review dedicated to nanofluid-based DASC for both concentrating and non-concentrating collectors is provided. The key findings and the challenges to be overcome toward promoting the development of nanofluid-based DASC for SHIP applications are discussed.

KEYWORDS

Solar Energy; Direct Absorption Solar Collector (DASC); Nanofluid; Solar heat for industrial processes (SHIP); Concentrating and non-concentrating technologies

HIGHLIGHTS

- Parabolic trough collector is the leading technology for SHIP installations.
- Nanofluid-based DASC improve the efficiency of conventional surface collector.
- Carbon nanoparticles show promising properties for direct absorption collectors.
- Low nanoparticle concentrations result in strong changes in absorption properties.
- The nanoparticle stability is highly affected by the fluid temperature.

Contents

1. Introduction

The International Energy Agency (IEA) reported in 2009 that 47% of the final energy used worldwide was related to heat demand [2]. The industry sector accounts for 32% of the global energy demand, and is currently the most energy consuming sector in the world [3]. 74% of the total energy demand in the industrial sector corresponds to heat (82 EJ), a three-fold larger value than the electricity demand. High temperature (>400 °C) heat represents 48% of the heat demand, while low and medium temperature (<400 °C) heat cover the remaining 52%. Modular size solar thermal collectors can supply low and medium temperature heat in industry, which would reduce the greenhouse gas emissions of the factory. Moreover, solar thermal energy systems can be hybridized with fossil or renewable fuels to supply heat on demand. The number of Solar Heat for Industrial Processes (SHIP) projects has increased considerably in the last 15 years, with at least 891 installations (791 MW_{th}) worldwide in 2020 [4]. Solar thermal collectors are still not affordable enough to represent a competitive alternative to fossil fuel-based heat, and intense research efforts are still required toward increasing the SHIP share in the industrial sector [5].

Nowadays, either concentrating or non-concentrating solar thermal collectors are used to convert the incident solar radiation into process heat. The incoming sunlight is absorbed at the receiver/absorber surface and transferred to a heat transfer fluid (HTF), usually water or thermal oil. Significant research efforts have been dedicated to the efficiency enhancement of surface collectors, either by increasing the heat transfer or by reducing heat losses with glass covers or vacuum chambers (see section III). The integration of micro or nano-size particles to the HTF in order to increase their thermal conductivity and improve the collector efficiency has also led to many recent publications [6–10].

Direct (or volumetric) absorption solar collectors (DASC) have recently been suggested as a way to enhance heat exchanges within conventional solar collectors, using a semi-transparent fluid acting both as an absorber and as a HTF [11,12]. Conventional HTF exhibit weak radiative properties, making them unsuitable for sunlight absorption. However, the addition of small-size particles offers a path for better tuning the absorption capability of the fluid. For example, carbonaceous micro-sized particles can improve the radiative properties of the fluid but suffer from settling or blocking of pumps due to their inappropriate size [13,14]. The dispersion of nanoparticles in the so-called nanofluids allows mitigating the settling and blocking issues commonly encountered with larger size particles, while enhancing the absorbing properties of the fluid. Nanofluid-based direct absorption solar collectors (NDASC) have three advantages over traditional surface collectors, 1) heat is absorbed volumetrically, which enhances internal heat distribution; 2) peak temperatures occur far from the walls, where most heat losses occur; and 3) NDASC offer versatility for hybrid photovoltaic-thermal (PVT) collectors, photo-chemistry, and other applications.

Most of the previously published reviews in the field of nanofluids for solar energy systems discuss their enhanced thermal conductivity as well as their suitability for hybrid concepts (PVT) with little focus on NDASC [14–25]. Trong Tam *et al.* [26] and Kumar *et al.* [27] reviewed NDASC collectors using carbon-based nanofluids and plasmonic nanofluids respectively. Rasih *et al.* published in 2019 two reviews centered in concentrating NDASC [28] and in numerical investigation advances of NDASC studies [29]. The review of Fu *et al.* [30] studies NDASC systems at medium-to-high temperatures, while that of Karami *et al.* [31] focus on low-temperature NDASC. The state-of-the-art of Gorji *et al.* [32] and Chamsa-Ard *et al.* [33] give a complete overview of advances in nanofluid properties and synthetization, and their use in NDASC collectors up to 2017. In this literature review, recent advances

in nanofluid-based DASC are presented together with a detailed analysis of SHIP applications and commercial surface collectors for future NDASC commercialization.

In this paper, we aim at gathering, classifying and discussing the most promising applications for low and medium temperature collectors (SHIP installations). Current commercial collectors used for SHIP installations are described and analyzed to better grasp the challenges likely to be met by NDASC toward commercialization, and a literature review dedicated to NDASC for both concentrating and non-concentrating collectors is provided. In the final section, the challenges to overcome toward promoting the development and the practical implementation of NDASC are discussed, and the key findings of this review are summarized.

Nomenclature

A	area (m^2)
C	concentration ratio
D	tube diameter (m)
I_0	incident radiation (W/m^2)
$I_{b,\lambda}$	blackbody spectral irradiance ($W/m^2.sr.nm$)
I_λ	spectral irradiance ($W/m^2.sr$)
k	absorption, scattering or extinction coefficient ($1/m$)
L	Length (m)
$\dot{m}$	mass flow rate (kg/s)
s	radiation beam direction vector
T	Temperature ($°C$)
ΔT	temperature difference ($°C$)
W	width (m)

Greek symbols

η	thermal or optical efficiency ($\%$)
λ	wavelength (nm)
ϕ	scattering phase function
ω	solid angle (sr)

Subscripts

abs	absorption
aper	aperture
ext	external
in	inlet; inner (diameter)
opt	optical
out	outlet
rec	receiver
sca	scattering
th	thermal

Acronyms

CPC	Compound Parabolic Concentrator
DAPTC	Direct Absorption Parabolic Trough Collector
DASC	Direct Absorption Solar Collector
DNI	Direct Normal Irradiance
ETC	Evacuated Tube Collector
FPC	Flat Plate Collector
HTF	Heat Transfer Fluid
LFC	Linear Fresnel Collector
MWCNT	Multi-Wall Carbon Nano-Tube
NDASC	Nanofluid-based Direct Absorption Solar Collector
PDC	Parabolic Dish Collector
PTC	Parabolic Trough Collector
PV	Photovoltaic cell
PVT	Hybrid Photovoltaic-Thermal collector
RTE	Radiative Transfer Equation
SHIP	Solar Heat for Industrial Processes
SWCNH	Single-Wall Carbon Nano-Horns
vol%	volume fraction ($\%$)
wt%	weight fraction ($\%$)

2. Solar Heat for Industrial Processes

Figure 1 shows the heat demand distribution by temperature range, for several key industrial sectors worldwide [34]. In most sectors, more than 80% of the total heat demand is associated with low and medium temperature heat, a temperature range particularly suited for SHIP plants (the mining and quarrying, as well as the food and tobacco industries showing the highest potential). In the case of the chemical sector, 50% of the heat demand could be supplied with a SHIP plant, but a hybrid installation is necessary to provide the high temperature heat demand. For the non-metallic and basic metals sectors, classical SHIP plants are not suitable due to the discrepancy in the typical operating temperatures of the SHIP plants and the metallurgical processes involved in these industries. This latter is an open field for research and innovation.

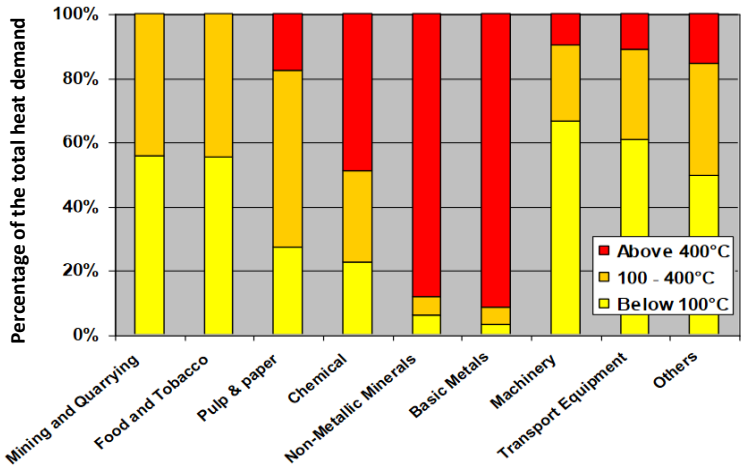

Figure 1: *Temperature level of the industrial heat demand by industry sector. Reprinted from Ref.* [34] *with permission from the author.*

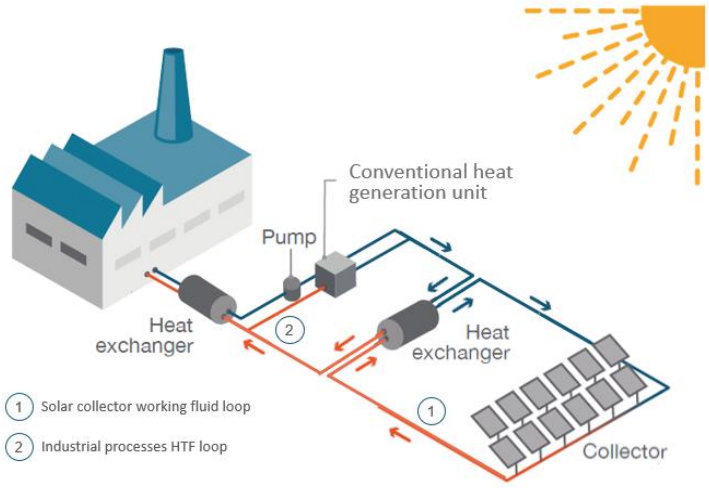

Figure 2: *Scheme of the general structure of a hybrid SHIP installation. The scheme is based on the figure from the Solar Payback report* [35].

Conventional industrial heating systems use a HTF closed circuit that supplies heat to the different processes [36]. The most common standard HTF used for low (≤100 °C) and medium temperature (100-400 °C) heat demand are liquid water, steam, and oil. Solar thermal collectors also use these fluids as HTF, which is a major advantage for the integration of solar energy in industrial plants. There are currently two possible integration solutions: 1) direct coupling of the solar field with the general HTF loop of the factory via a heat exchanger (**Figure 2**); and 2) coupling of the solar field with a particular single process of the factory. In most SHIP plants, solar energy is coupled with another thermal energy source (forming a *hybrid* installation) because of the intermittent nature of solar

energy (**Figure 2**) [37]. Solar energy can supply most of the heat demand while the conventional heat generation unit is run to provide the unmet heat demand (either because the solar power contribution is not sufficient, or because the heat temperature is too low).

In a SHIP plant, the land footprint of the solar field may constitute a serious hurdle. Rooftop solar collectors offer a relevant solution to the space availability problem, but may suffer from excessive wind loads, impeding their practical implementation. The rooftop area may not be sufficient to supply all the heat demand and additional ground areas can be required. The solar resource is largely determined by the location of the factory: potential market areas for SHIP include North African countries, the Middle East, the Mediterranean countries, Australia, USA, India, China, and South America [37]. Nevertheless, SHIP installations may also be worth implementing in countries with lower solar irradiation, and could contribute reducing the environmental impact and the energy consumption in these locations as well (as illustrated by Germany, which currently hosts the largest number of SHIP plants in Europe (33 projects), despite its limited solar resource [38]).

Table 1: *SHIP projects by industry sector* [36,38–41]. *Technology abbreviations refer to: parabolic trough collector (PTC), flat plate collector (FPC), linear Fresnel collector (LFC), evacuated tube collector (ETC), and parabolic dish collector (PDC).*

Industry sector	Country	Year	Company	Process	Technology	T (ºC)
Food	Mexico	2013	Durango dairy	Boiler preheating	PTC	20-95
	Mexico	2014	Nestle Dairy Plant	Pasteurization	PTC	80-95
	India	2018	Hatsun Dairy	Drying	PTC	-
	Czech Republic	2003	PETA Bohemia Pekarna Sobeslav	Bakery	FPC	10 - 90
	Switzerland	2012	Emmi Dairy Saignelsgier	Drying processes	PTC	140-180
	Italy	2015	Nuova Sarda Industria Caaseria	Process heating	LFC	200
	Spain	2013	Papes Safor	Boiler preheating	PTC	200-250
	Greece	1999	Alpino SA	Boiler preheating	FPC	20 - 70
	Portugal	1987	Knorr Best Foods	Tools washing	FPC	40 - 45
	Spain	2015	Grasas del Guadalquivir	Process heating	LFC	130
	USA	2008	Frito Lay	Steam for heating	PTC	243
Breweries	Mexico	2014	Quesos La Doñita	Pasteurization	PTC	60-95
	Cyprus	2021	KEAN soft drinks	Steam for cleaning, sterilization and pasteurization	PTC	188
	Germany	2009	Hofmuhl Brewery	Bottle washing	ETC	20-110
Textile	China	2007	Daly Textile	Dyeing process	FPC	55
	China	2011	Jiangsu Printing & Dyeing	Preheating: printing & dyeing	ETC	50
	Germany	-	Meiser Textile	Process heating	PTC	140
Fabricated Metal	Germany	2010	Alanod	Aluminium process	PTC	143
	France	-	Viessmann Faulquemont	Cleaning bath	ETC	60
	Portugal	2014	Silampos S.A.	Drying products	PTC	50-160
Medical	India	2014	PSG Hospitals	Laundry and sterilization	PTC	150
Paper	Canada	2014	Parc Solaire Alain Lemaire	Boiler pre-heating	PTC	120-140
	India	2011	B.S. Paper Mill	Process heating	PDC	90-100
Automobile	India	2015	Harite Seatings Systems Limited	Cleaning automobile parts	ETC	55-60
	India	2010	Mahindra Vehicle Manufacturers	Washing engine components	PDC	120
Pharmaceutical	Egypt	-	El Nasr Pharmaceutical	Process steam	PTC	173

	India	2014	Abbott Healthcare	Boiler heating	PDC	-
	Spain	-	Covex	Process heat	PDC	50-90
Chemical	China	2016	Procter & Gamble	Boiler heating	PTC	130
Mining	South Africa	2011	Xstrata Elands Mine	Cleaning	ETC	60

SHIP are particularly developed among the food sector, with India and Mexico hosting the largest number of SHIP installations [38,42] (**Table 1**). In 2013, 61% of the Indian solar thermal capacity was used for industrial processes and community cooking (208 installed projects in 2017) [37,42]. In Mexico, 83 SHIP projects were installed in 2020, 48 of which provide heat to the food sector [38]. A direct coupling integration method is preferred among SHIP plants with most plants working at temperatures between 60-150 °C.

International organizations and governments are pushing forward the development of SHIP projects at a national and international level. The International Energy Agency (IEA) and SolarPACES founded the Solar Heating and Cooling (SHC) program to promote solar energy for low and medium heat demand [43]. Among their projects, "Task 64/IV – Solar Process Heat" is centered in SHIP projects and their development, as well as in creating a SHIP market guideline [44]. In Europe, the Solar Heat Europe association strives for the growth of SHIP installations by analyzing market statistics and by working with EU policymakers to increase the share of solar heating technologies in the European economy [45].

3. Commercial solar thermal collectors

Solar thermal collectors can be classified into two groups: non-concentrating (or stationary) and concentrating collectors. Non-concentrating collectors involve the absorption of the incident radiation by the absorbing surface (or volume) directly exposed to the solar flux. Concentrating collectors use reflecting mirrors to intercept and focus the incident solar radiation onto a smaller area, and require sun tracking to efficiently collect and concentrate solar radiation (unlike non-concentrating collectors, concentrators only exploit Direct Normal Irradiation (DNI)).

3.A.- Non-concentrating collectors

The two main non-concentrating technologies are Flat Plate Collectors (FPC) and Evacuated Tube Collectors (ETC) [37], both technologies using water as HTF due to their low working temperature [46]. **Table 2** presents the main characteristics of the two types of collectors.

3.A.1.- Flat plate collectors (FPC)

FPC convert the incident solar radiation into heat via an absorbing black plate coated with a selective absorbing material. The absorbed heat is then conducted through copper pipes, and collected by the working fluid flowing inside [36]. Conventional FPC operating temperatures range from 20 °C to 80 °C [5,46] with a 60% average collector efficiency. Integration of a double-glass cover or a vacuum chamber can level the maximum operating temperature up to 150 °C [5] and the collector efficiency up to 70% in the 20-80 °C temperature range [2,5]. FPC are used in the food and textile sectors (see **Table 1**) [5,36,38,47].

3.A.2.- Evacuated tube collectors (ETC)

An ETC consists of a row of parallel evacuated tubes absorbing independently the incident solar irradiation. The tubes are composed of one or two glass layers, a vacuum chamber, a metallic absorbing layer with a selective coating, and fluid tubes containing the working fluid [46,49] (see [5,46,48] for more information about these designs). FPC performances are examined in [37,46,50]. Standard ETC work at temperatures up to 120 °C with a collector efficiency of ~60%, however new generations allow temperatures of 170 °C or 180 °C to be reached [2,5,37,46]. For further information, the Solar Rating & Certification Corporation provides a detailed comparison of most commercialized tubular solar collectors [51].

Table 2: *Summary of non-concentrating solar thermal collectors.*

Collector [Ref.]	Absorber	Dimension	Temperature	Advantages (Adv.) and Disadvantages (Disadv.)
FPC [1,4,27–29,36, 41]	Planar	-	50-120 °C	Adv.: ◦ Light and affordable. ◦ Main technology for low-temperature SHIP (40-90 °C). Disadv.: ◦ Low efficiencies (<60 %) beyond ~80 °C.
ETC [2,5,37,46,50,51]	Tubular	D_{tube} = 50-100 mm	60-180 °C	Adv.: ◦ Large temperature range (up to 120 °C) with nearly constant efficiency (60 %). ◦ Popular for residential heating and cooling. Disadv.: ◦ More expensive than FPC. ◦ Less popular than FPC for low-temperature SHIP and than PTC for medium-temperature SHIP.

3.B.- Concentrating collectors

Two distinct families of optical concentrators can be distinguished based on the tracking strategy followed. One-axis tracking systems involve tracking the course of the sun along one single axis (east-west or, less commonly, north-south [35,52,53]), the most popular axis tracking systems to date being parabolic trough collectors (PTC) and linear Fresnel collectors (LFC). Two axes sun-tracking offer an extra degree of freedom in the quest of high concentration ratios. Two main technologies dominate this family of systems: parabolic dish collectors (PDC) and solar towers (ST). Solar towers use a field of heliostats (mirrors) to concentrate the incident radiation on a fixed-focus central receiver located atop a tower. This technology being solely used for electricity generation at high temperatures (up to 560 °C for molten salt solar power towers), it will not be addressed in this review. PTC, LFC, and PDC generally use either water, steam or thermal oil as HTF. **Table 3** summarizes the main characteristics of the three concentrating collectors.

3.B.1.- Parabolic trough collectors (PTC)

PTC use cylindrical shape reflectors to focus direct solar radiation onto the moving linear receiver situated at the collector focus (focal line) (**Figure 3.a**). The receiver consists of an evacuated glass tube encompassing an inner metal tube coated with a selective material [52,54]. Small and medium PTC, whose typical dimensions are summarized in **Table 3**, are able to work at temperatures comprised between 100 °C and 300 °C [37] and are widely used in SHIP plants for medium temperature heat applications [4,38], residential heating and heat-driven refrigeration and cooling [54].

3.B.2.- Linear Fresnel collectors (LFC)

LFC use horizontally aligned flat or quasi-flat mirrors to track the sun and reflect solar energy towards a fixed focus where the receiver is located (**Figure 3.b**). Unlike PTC, standard LFC are not able to concentrate sunlight on a small-size focal line due to the planarity of the reflectors and, therefore, use cavity receivers with secondary reflectors [53,55]. As PTC, large LFC reach around 400 °C and are used for electricity generation [56,57], while medium size LFC (see **Table 3**) have an operating temperature range of 80-300 °C and supply heat for SHIP plants, residential heating and heat-driven refrigeration [5,37–39].

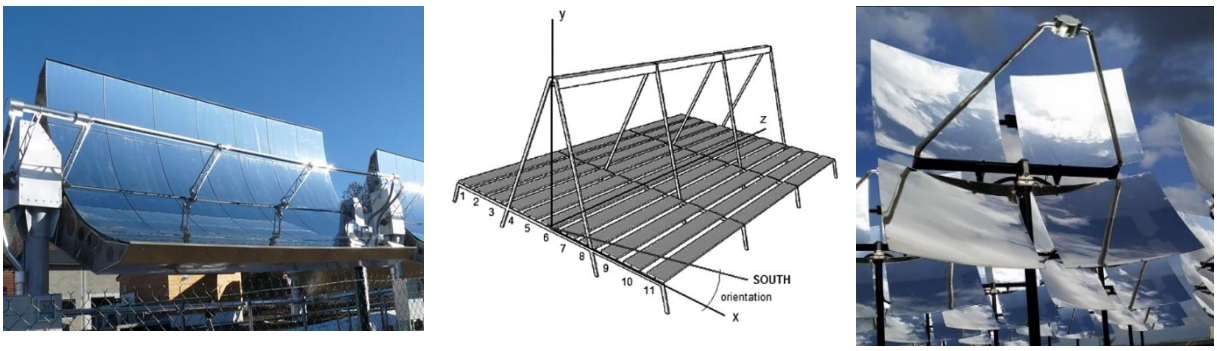

(a) (b) (c)

Figure 3: *Medium-size concentrating solar thermal collectors: (a) a PTC (PROMES laboratory); (b) scheme of a LFC; and (c) the TCT-RED PDC proposed by Thermal Cooling Technology®. Figures (a), (b) and (c) reprinted from Ref.* [58] *with permission from PROMES, Ref.* [59] *with permission from Elsevier and Ref.* [40] *with permission from Thermal Cooling Technology®, respectively.*

3.B.3.- Parabolic dish collectors (PDC)

PDC consist of a parabolic reflector dish focusing sunlight onto the receiver, consisting in a cylindrical cavity with an absorbing plate. Several PDC designs can be found in the market, such as the ARUN dish [60], the Scheffler dish [61,62] or the TCT-RED proposed by Thermal Cooling Technology®

(**Figure 3.c**) [40]. In India, PDC is the leading solar technology supplying heat for community cooking and industrial process heat, with 88 projects installed during 2017 [64]. Outside India, PDC for heat generation are not very developed, with only a few SHIP projects using PDC in Spain or Argentina [40,65,66].

Table 3: *Summary of concentrating solar thermal collectors.*

Collector [Ref.]	Concentrator (1)		Receiver (2)	Temperature	Advantages (Adv.) and Disadvantages (Disadv.)
(1) Length (L), width (W), aperture area (A_{aper}), and concentrating ratio (C); (2) Inner diameter (D_{in}) and outer diameter (D_{out})					
PTC [4,38,67–74]	Linear	L = 2 - 5 m W = 1 - 3 m C = 15 - 40	Tubular D_{in} = 20 - 80 mm D_{ext} = 80 - 140 mm	100-300 °C	Adv.: ◦ High optical and thermal efficiencies. ◦ Most popular technology for medium temperature SHIP (100-250 °C). Disadv.: ◦ Receiver, which entails important constraints for junctions.
LFC [5,37–39,75–81]	Linear	L = 3 - 20 m W = 1 - 7 m C = 10 - 25	Cavity with a secondary reflector	80-300 °C	Adv.: ◦ Higher land-use efficiencies and lower wind loads than PTC, important constraints in rooftop installations. ◦ Flat reflectors are more affordable than parabolic reflectors. ◦ Fixed receiver. Disadv.: ◦ Lower optical efficiency than PTC. ◦ Technology less developed than PTC.
PDC [40,60–66]	Point focus	A_{aper} = 16-100 m² C = 100-250	Cavity	100-300 °C	Adv.: ◦ Better optical efficiencies than PTC and LFC. ◦ Well known technology with a large number of SHIP installations in India. Disadv.: ◦ Highly affected by wind loads.

3.C.- Conclusion

Despite their affordability, non-concentrating collectors suffer from low efficiencies above 150 °C, a temperature level beyond which concentrating collectors demonstrate higher performances. PDC suffer from high wind loads, an important parameter when SHIP rooftop installations are intended. LFC and PTC have the advantage of a higher working temperature range than ETC but strongly depend on the typical DNI of the location. In conclusion, ETC are better suited for SHIP installation in locations characterized by a low annual average DNI, while LFC and PTC are more favorable for locations with high DNI and offer a higher heat temperature range. Considering the use of nanofluids for DASC, linear tubular collectors are more favorable than point focus or planar collectors owing to the progressive linear absorption and the fluid flow direction. Planar collectors, like nanofluid-based FPC, may be favorable for hybrid PVT systems with the nanofluid acting as an optical filter. Further detail regarding non-concentrating and medium-size collectors for SHIP applications can be found in the following articles and reports [5,46,48,54,57,82].

4. Nanofluid-based direct absorption solar collectors (NDASC)

In this section, the underlying physical principles of the NDASC are discussed, and the main nanoparticles properties as well as their effect on NDASC operation are described. A wide range of studies have already discussed how the integration of nanofluids may improve the absorption properties of these solar collectors, focusing solely on the optical properties of the nanofluids. Here, we aim at extending our analysis beyond these aspects and discuss literature outcomes related to the volumetric absorber itself, both on numerical and experimental grounds.

The absorber container (plate or tube) as well as the absorbing medium, constitute two key elements differentiating surface collectors from DASC. In a DASC, the radiation is absorbed in the volume of the HTF rather than at the surface of the collector (as illustrated in **Figure 4**). Consequently, the absorber container must be transparent to solar radiation.

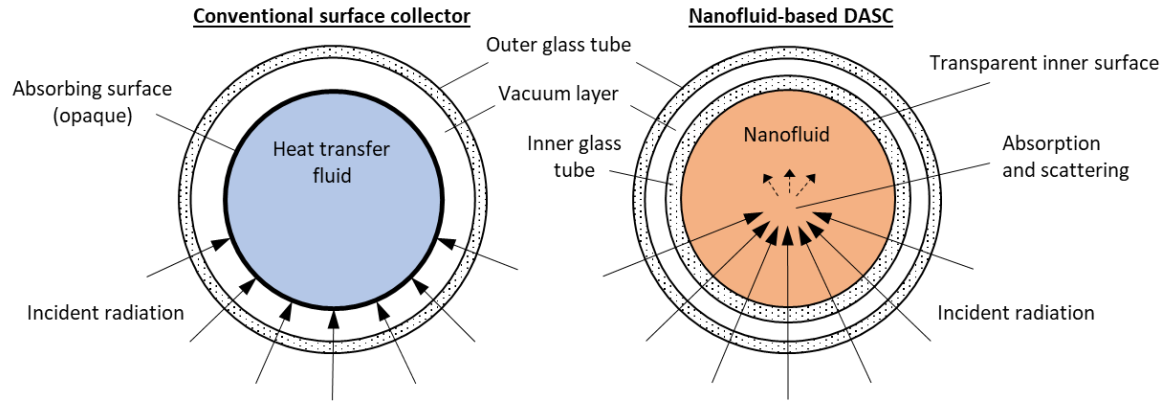

Figure 4: *Diagram of the optical principle of a conventional tubular surface collector and a nanofluid-based tubular DASC.*

4.A.- Physical principles and properties of nanofluids

Since solar radiation is absorbed in the volume of the HTF, the extinction of sunlight through the fluid must be understood. The Radiative Transfer Equation (RTE) defines the variation of the radiation intensity due to absorption, scattering, and emission of the medium (Eq. 2):

$$\frac{d}{ds}I_\lambda(s) = -k_{\mathrm{abs},\lambda}I_\lambda(s) - k_{sca,\lambda}I_\lambda(s) + k_{abs,\lambda}I_{b,\lambda}(s) + \frac{1}{4\pi}\int_{4\pi} k_{sca,\lambda}I_\lambda(s)\phi_\lambda(\omega' \to \omega)d\omega' \quad (2)$$

where I_λ is the spectral radiative intensity, λ the wavelength, k_{abs} the absorption coefficient, k_{sca} the scattering coefficient, $I_{b,\lambda}$ the blackbody spectral radiative intensity, ϕ_λ the scattering phase function, and ω the solid angle. The parameter "s" represents the distance travelled by the radiation beam through the medium. The most common assumption to solve the RTE considers the scattering coefficient of the nanofluid negligible compared to the absorption coefficient. In addition, as the working temperatures of DASC are relatively low, the emission term of the RTE can generally be neglected too. These assumptions lead to a well-known form of the RTE, the Beer-Lambert equation (eq. 3), which points out the exponential decrease of the solar irradiation intensity along its propagation path in the medium.

$$I_\lambda(s) = I_\lambda(0)exp\left(-k_{abs,\lambda}\cdot s\right) \quad (3)$$

Several methods are commonly used to characterize the absorption properties of the nanofluid depending on the particle type, shape and mean size. The Rayleigh scattering approximation is the most accurate and popular solution method [1,12,26,31,32,83–94], other methods such as the Mie scattering theory [92,95–97] or the Maxwell-Garnett theory being less used [91,98]. Among metal nanoparticles, gold (Au), silver (Ag), copper (Cu), and aluminum (Al) show the best optical properties

for NDASC. Metal oxides showing the best potential for direct absorption applications are silica (SiO_2), iron oxide (Fe_3O_2), copper oxide (CuO), and alumina (Al_2O_3). Carbon-based nanoparticles most commonly used for NDASC are carbon nanotubes (CNT) (single-walled or multi-walled), single-walled carbon nanohorns (SWCNH), and graphene nanoplatelets. The performance of graphene oxide and reduced-graphene oxide nanoparticles has also been investigated [99,100]. The nanoparticles' shape and size are evaluated microscopically and spectroscopically with well-known methods such as scanning electron microscopy (SEM), transmission electron microscopy (TEM), or atomic force microscopy (AFM) [101–108]. Three base fluids are essentially used: water, ethylene glycol and thermal oils. Further information about the thermophysical and optical properties of nanofluids for DASC can be found in references [109–115].

4.B.- Non-concentrating NDASC

The main characteristics and performances of non-concentrating NDASC studies are summarized in **Table 4** chronologically. The following section will discuss these findings into more details.

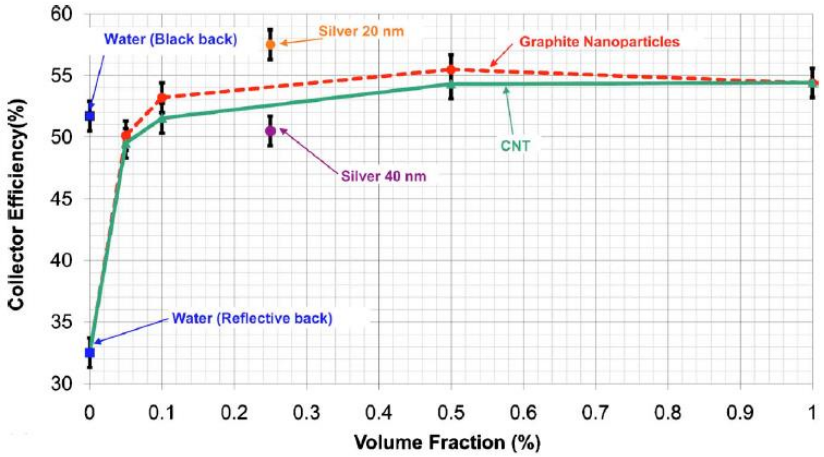

Figure 5: *Experimental collector efficiencies as a function of the vol% for NDASC with different nanoparticles dispersed in water. The surface collector is plotted under the name "Water (black back)". Reprinted from Ref.* [13] *with the permission of AIP Publishing.*

In 1975, Minardi and Chuang [11] studied experimentally for the first time the performance of a volumetric planar collector using a black Indian ink and found collectors' efficiencies up to 80%. Their work underlined the expected advantages of fluid-based DASC over conventional planar collectors: temperature distribution, lower heat losses, versatility and lower cost. With the rise of nanomaterials science, a broad range of studies has been dedicated to the optical characterization of nanofluids as well as their possible integration in solar thermal collectors. Tyagi *et al.* [12] were the first to numerically study the efficiency of a 2D planar NDASC incorporating Al nanoparticles dispersed in water. Their model predicts efficiencies up to 80% with a 3.0% nanoparticle volume fraction (vol%) and a 1.2 mm collector thickness, representing a 10% efficiency increase relative to conventional FPC, and laid the groundwork for future studies on numerical NDASCs.

Lee *et al.* [95] and Cregan and Myers [84] studied numerically Al nanoparticles dispersed in water with lower concentrations, between 0.0005 and 0.02 vol%, and demonstrated relatively high efficiencies despite the low concentration levels and collector heights (see **Table 4**). Among metals, Ag nanoparticles have been widely studied for NDASC as a result of their high absorption properties at low volume fractions [13,85,86,116–118]. Otanicar *et al.* [13,116] demonstrated higher efficiencies with Ag particles rather than carbon nanotubes or graphite particles, even at lower Ag particle

concentrations (0.25 vol%) (**Figure 5**). However, later numerical and experimental studies [85,86,117] aiming at comparing Ag, graphite and magnetite nanoparticles at low concentrations (less than 0.004 vol%), shown higher thermal efficiencies with magnetite particles, followed by graphite. This discrepancy outlines the high impact of the particle size, the particle volume fraction and the collector height on efficiency and outlines the compromise that should be made between these parameters. Other metal particles, such as Cu, Au, Fe or Ni, have also been studied numerically and spectrophotometrically, and demonstrated interesting characteristics for direct absorption applications [119,120,110,121–123], despite the limited range of experimental studies available. Metal-oxides such as CuO, SiO_2, Al_2O_3 or TiO_2 demonstrated promising absorbing properties but also lower efficiencies than their metal or carbon based counterparts [96,124–127]. Nevertheless, metal-oxides can be relatively easily coupled with metal or carbon particles to create hybrid nanofluids.

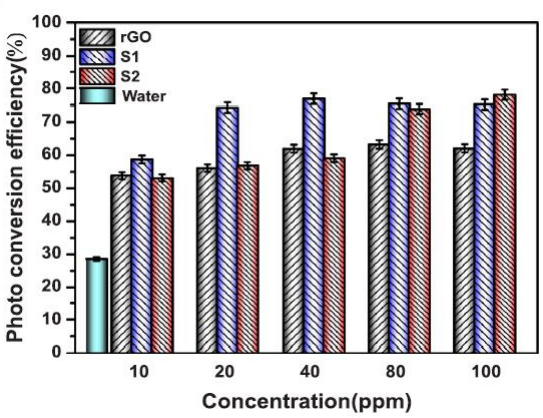

***Figure 6**: Photo-thermal conversion efficiencies as a function of the nanoparticle concentration for the different samples: water, reduced-graphene oxide (rGO), plasmonic fluid with 0.15g of Ag (S1), and plasmonic fluid with 0.30g of Ag (S2). Reprinted from Ref.* [99]*, an open access article not-requiring permission.*

As outlined by several authors, controlling the particle size and configuration of metal nanoparticles, e.g. core-shell particles, could lead to more efficient absorbing nanofluids thanks to the plasmon resonance phenomenon [128,129]. Lee *et al.* [95,130] studied analytically the efficiency of a planar NDASC incorporating core-shell nanoparticles, namely SiO_2 core and Au shell, dispersed in water. The authors outlined that scattering phenomena needs to be considered when plasmonic particles are used, as the surface plasmon enhances both absorption and scattering. The optical analysis emphasizes the absorption wavelengths variation with the nanoparticle configuration (core and shell dimensions). By selectively choosing the core-shell configuration of the particles and their relative fraction in the solution, the authors obtained a nanofluid demonstrating higher performances in comparison with Al-based nanofluid. Mehrali *et al.* [99] demonstrated higher thermal efficiencies with graphene-silver hybrid plasmonic nanoparticles than with reduced-graphene oxide particles, using water as based-fluid (**Figure 6**). The experiment analyzed the photo-thermal conversion with a static (no-flow) sample of the nanofluids, and thus results should be verified with under flow conditions. Further information about plasmonic particles used in DASC can be found in Mallah *et al.* [112,131] and Kumar *et al.* [27] reviews. The book recently published by Zafar Said, *Hybrid Nanofluids* [115], gives a complete overview of the history of hybrid nanofluids, their preparation and their potential applications. Plasmonic and hybrid nanofluids constitute promising options toward enhancing the absorption properties of common nanofluids for NDASC at low volume fraction. However the complexity of their synthesis and their high production cost could impede their future commercialization [27].

Carbon-based nanofluids have been considered as the most promising working fluid for NDASC owing to their outstanding thermal and optical properties [26,111]. Otanicar *et al.* [13,116] characterized both graphite and carbon nanotubes, and showed slightly higher performances for the former (**Figure 5**). Both multiwalled (MWCNT) or single-walled (SWCNT) carbon nanotubes are the most commonly used carbon-based nanoparticles for NDASC, efficiencies up to 89% were obtained with relatively low concentrations (less than 100 ppm) [13,87,132,133]. Luo *et al.* [96] demonstrated higher efficiencies with graphite, relative to Al_2O_3 nanoparticles, using a 50 times lower volume fraction, both on theoretical and experimental grounds. Similarly, Gorji and Ranjbar [85,86,117] revealed a 30% improvement in the thermal efficiency of graphite-based nanoparticles, in comparison with Ag nanoparticles, that are currently considered as one of the most promising metal nanoparticles for NDASC. The new promising 2D carbon-based nanoparticle, graphene, has shown enormous potential for NDASC with over 90% efficiencies at low concentrations (0.02-0.005 weight fraction (wt%)) [100,134,135]. Graphene oxide and reduced graphene oxide show promising absorption properties as well as versatility for hybridization with metal nanoparticles such as silver [99,100]. Further experimental studies are still needed to determine the optimal graphene volume fractions as well as the optimal working conditions (flow rate, fluid temperature, etc…). The analysis provided by Khullar *et al.* [111] offers a full overview of the thermal and optical properties of the principal nanoparticles used in NDASC, and concluded that carbon-based nanofluids are the most suitable candidates. Further comparisons between carbon nanofluids, plasmonic, and hybrid nanofluids including all aspects of the technologies (see **section 5**) are still required to determine the best volumetric absorbers today.

As revealed in **Table 4**, the most widely used base fluid for non-concentrating NDASC is water. Owing to the moderate temperature increase, water is the most affordable and practical base fluid. The influence of the base fluid on the performance of the collectors is scarcely addressed in the literature. The absorption properties of water-based nanofluids incorporating carbon nanoballs were shown to be slightly higher than ethylene glycol-based samples [136], which was confirmed numerically by Moradi *et al.* [137] considering a water and an ethylene glycol based NDASC using SWCNH. Thermal oils and glycols may offer an advantage over water when temperatures beyond 100 °C are attaint due to their higher boiling temperature, issue addressed for concentrating NDASC in the next subsection.

The role of the particle size was investigated by several authors: Tyagi *et al.* [12] suggested that the collector efficiency is weakly correlated with particle size, a conclusion supported by other researchers in later studies [31,83,84,90,110]. However, Otanicar *et al.* [116] and Chen *et al.* [119] noticed an efficiency drop inversely correlated to particle size, for both Ag and Au nanoparticles. He *et al.* [138] outlined that the heat transfer properties of nanofluids are improved for decreasing particle size, while the optical properties are slightly worsened: such trends could explain the discrepancies in the conclusions reached by these authors. It can be concluded that the particle size has a limited impact on the optical properties of DASC nanofluids for particle size below 100 nm. However, since the heat transfer properties are enhanced for decreasing particle size [139], smaller particles might be preferred for systems involving large temperature gradients.

Most metal-based DASC studies involve spherical-shaped nanoparticles, since metal particles are mostly spherical and modeling theories are based on the spherical assumption (Rayleigh scattering approximation, Mie scattering theory, etc…). Carbon-based nanofluids incorporate tubular or flat shaped nanoparticles (CNT or graphene for example), which makes them preferable over metals or oxides as their larger surface area increase the heat transfer rate between the particles and the base

fluid [19,26,140]. Morphology studies aiming at understanding how the shape of the particles affect the system performance were published for DASC system involving plasmonic or hybrid nanofluids [27,95,130,131,141–143]. As outlined by Mallah *et al.* [131], the nanoparticle shape influences the spectral absorption of the nanofluid, offering the possibility of creating blended nanofluids with increased absorption properties, and thus higher NDASC performances, by carefully choosing the particle shape and volume fraction.

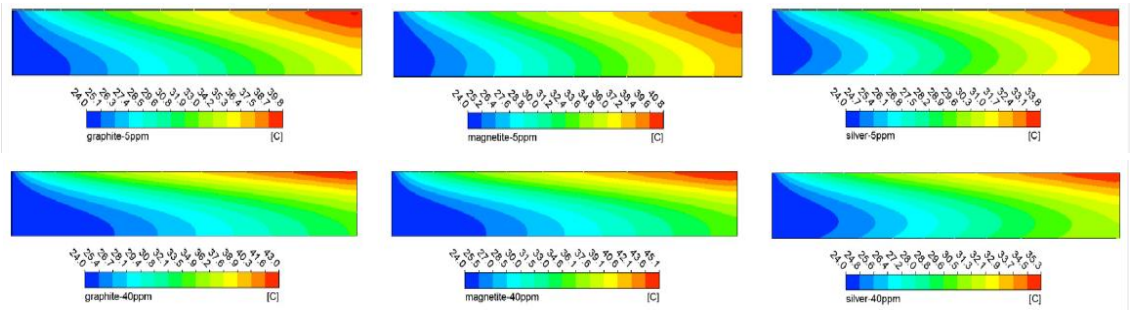

***Figure 7**: Temperature contours for three nanofluids (graphene (50 nm), magnetite (15 nm), and silver (20 nm)) with two different nanoparticle's concentration, 5 ppm and 40 ppm. The simulated collector is 12.1 cm long, 5 cm wide, and 2 cm high. Reprinted from Ref.* [86] *with permission from Elsevier.*

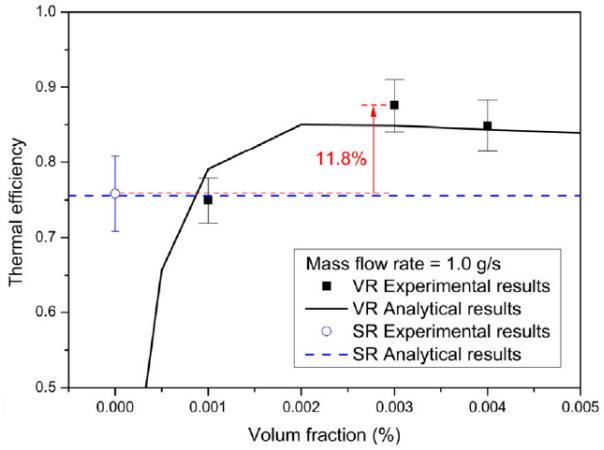

***Figure 8**: Thermal efficiency (analytical and experimental results) for the surface receiver (SR) and the volumetric receivers (VR) at different MWCNT vol%. Reprinted from Ref.* [133] *with permission from Elsevier.*

It is widely accepted that the two crucial parameters affecting the collector's performance are 1) the particle volume fraction and 2) the fluid depth (distance travelled by the incident light throughout the nanofluid). The absorption coefficient of a nanofluid increases with the particle volume fraction. However, as can be deduced from the Beer-Lambert's law (eq. 3), the absorbed radiation in a fluid varies exponentially with the fluid depth, resulting in a higher fraction of the incident radiation absorbed in the first fluid layers. Therefore, increasing the particle concentration over a specific threshold value can lead to the complete absorption of the incident radiation on the first nanofluid layers, and result in temperature contours similar to those of conventional surface collectors. **Figure 7** from Gorji and Ranjbar [86] reflects the increase of the top layer temperatures proportionally with the particle volume fraction. Higher temperatures in the top fluid layers would induce higher heat losses and negatively impact the collector efficiency. A compromise between the volume fraction and the collector's depth needs to be found to determine the optimal nanofluid, which differs for each particle-type and working conditions, as outlined in **Figure 5, Figure 6** and **Figure 8** [13,99,133,144]. The collector and thermal efficiencies of various NDASC are given in **Table 4**. Three important limitations currently preventing NDASC commercialization are nanofluid stability, production cost and environmental impact (see **section 5**): these parameters appear to be strongly penalized by the

increase in the nanoparticle volume fraction, and future research work aiming at optimizing these parameters for lower volume fraction nanofluids should thus be pursued.

Similarly to conventional surface collectors, the efficiency of a NDASC is affected by the increase of the fluid temperature due to higher heat losses [86,87,100,126,134]. The temperature increase may also affect the nanofluid stability due to the temperature-dependence of the surfactant degradation, organic compounds used to improve chemically the stability of nanofluids, which constitutes a major factor of nanofluid instability and reduction of absorption properties (refer to **section 5** for further information about the stability challenge). By increasing the nanofluid flowrate, the time during which the fluid is exposed to radiation is reduced, which lowers the fluid temperature and improves the thermal efficiency of the collector [86,87,135]. Thanks to the progressive absorption of radiation along the fluid volume, NDASC are not constrained by the flow regime unlike surface collectors, which need high Reynolds number regimes for increasing the convective part of the heat transfer fluid. Yet, Struchalin *et al.* [145] demonstrated that the deposition efficiency (capability of nanoparticles to deposit in the collector's inner surface) decreases from 49% in a laminar flow to 1-2% in a turbulent flow, making high Reynolds number regimes preferable. The sensitivity of nanofluids to the flow regime is strongly linked to the elaboration method (base fluid, particle properties, additives). The investigation carried by Bhalla *et al.* [146] provides a comprehensive understanding of the influence of different working parameters (mass flow rate, incident radiation, collector depth, etc…) on the collector efficiency using amorphous carbon-based nanofluids. Studies summarized in **Table 4** demonstrate the capability of NDASC to outperform surface planar collectors, with efficiencies enhanced by 10-15 % using low particle volume fraction. Novel NDASC using porous materials [147] or in between absorbing plates [148] can also be found in **Table 4**.

Table 4: *Summary of non-concentrating NDASC reviewed.*

NON-CONCENTRATING NDASC									
Authors (year) [ref.]	**Approach**			**Nanofluid**				**Results**	
	Num./Exp.	Geometry	Fluid depth	Nanoparticles	Base Fluid	Size	Concentration	Temperature	Efficiencies
Otanicar *et al.* (2009) [116]	**Numerical**	Planar	0.3 mm	Graphite	Water	D = 30 nm	0.4-1.0 vol%	-	η_{col} = 71% - 69%
				Ag		D = 10 - 30 nm	0.1 vol%	-	η_{col} = 39.8% - 41.5%
Tyagi *et al.* (2009) [12]	**Numerical**	Planar	1.2 mm	Al	Water	D = 5 nm	3 vol%	-	η_{col} = 80%
Otanicar *et al.* (2010) [13]	**Num./Exp.**	Planar	0.15 mm	Graphite	Water	D = 30 nm	0.5 vol%	-	η_{col} = 55.5%
				CNT		D = 6 - 20 nm	0.5 vol%	-	η_{col} = 54.0%
				Ag		D = 20 - 40 nm	0.25 vol%	-	η_{col} = 50.5% - 57.5%
Lee *et al.* (2012) [95]	**Numerical**	Planar	1.5 mm	Au-SiO_2 (Shell-Core)	Water	SiO_2: D = 20 - 55 nm Au: D = 3 - 10 nm	0.02-0.1 vol%	ΔT = 45 °C	η_{col} = 70.0%
				Al		D = 5 nm	0.02-0.1 vol%	ΔT = 25 °C	η_{col} = 42.0%
Kundan and Sharma (2013) [124]	**Experimental**	Planar	-	CuO	Water	D = 80 nm	0.005 vol%	-	η_{col} = + 6% vs a FPC
							0.05 vol%	-	η_{col} = + 4% vs a FPC
Ladjevardi *et al.* (2013) [83]	**Numerical**	Planar	100 mm	Graphite	Water	D = 30 nm	0.0025-0.000025 vol%	-	-
Verma et Kundan (2013) [125]	**Experimental**	Planar	-	Al_2O_3	Water	D = 40 nm	0.05 vol%	-	η_{col} = +3% - +5% vs a FPC
Karami *et al.* (2014) [150]	**Numerical**	Planar	3 - 5 mm	SWCNH	Water	-	0.001-0.05 g/l	ΔT = 0.1 °C	η_{col} = 18.0% - 87.0%
Lee *et al.* (2014) [132]	**Num./Exp.**	Planar	7.9 mm	Conventional FPC				-	η_{col} = 75.4%
				MWCNT	Water	D = 20 - 30 nm L = 10 µm	0.005-0.02 vol%	-	η_{col} = 41.0% - 90.0%
Luo *et al.* (2014) [96]	**Num./Exp.**	Planar	25 mm	TiO_2, Ag, Cu, SiO_2, CNTs	Texatherm oil	D = 10 - 50 nm	0.01-0.1 vol%	-	-
				Al_2O_3		D = 20 nm	0.5 vol%	T_{out} = 52 °C	η_{col} = 117.5% vs a FPC
				Graphite		D = 35 nm	0.01 vol%	T_{out} = 50 °C	η_{col} = 122.7% vs a FPC
Cregan and Myers (2015) [84]	**Numerical**	Planar	1 - 4 mm	Water				-	η_{col} = 3% - 5%
				Al	Water	D = 20 nm	0.0005 vol%	-	η_{col} = 25% - 50%
							0.006 vol%	-	η_{col} = 49% - 58%
Gorji and Ranjbar (2015) [85]	**Numerical**	Planar	10 - 20 mm	Graphite	Water	D = 30 nm	0.05; 0.5; 1.0 vol%	-	η_{th} = 49.0% - 58.0%
							0.1 vol%	T_{out} = 33 - 37 °C	η_{th} = 67.05% - 78.06%
Gupta *et al.* (2015) [126]	**Experimental**	Planar	6 mm	Al_2O_3	Water	D = 20 - 30 nm	0.001-0.05 vol%	-	η_{col} = + 20 - 40 % of water η
Liu *et al.* (2015) [134]	**Num./Exp.**	Tubular	50 mm	Graphene	[HMIM]BF_4	-	0.0005 wt%	T_{out} = 56 °C	η_{col} = 70% - 86%
							0.001 wt%	T_{out} = 77 °C	η_{col} = 55% - 83%

							0.002 wt%	-	η_{col} = 40% - 81%
							0.01 wt%	-	η_{col} = 24% - 75%
Moradi *et al.* (2015) [137]	**Numerical**	Tubular	44 mm	SWCNH	Water	D = 2 - 5 nm L = 30 - 50 µm	0.006 g/l ; 0.02 g/l	T_{out} = 23 - 25 °C	η_{col} = 62.5% ; 61.0%
					Ethylene Glycol		0.005 g/l ; 0.02 g/l	T_{out} = 23 - 28 °C	η_{col} = 51.5% ; 52.5%
Delfani *et al.* (2016) [87]	**Num./Exp.**	Planar	10 mm	Water				T_{out} = 36 °C	η_{col} = 60.3%
				Standard surface collector				T_{out} = 38 °C	η_{col} = 71.7%
				MWCNT	Water	D = 10 - 20 nm L = 10 - 30 µm	25-100 ppm	T_{out} = 37 - 40 °C	η_{col} = 77.6% - 89.3%
Gorji and Ranjbar (2016) [86]	**Num./Exp.**	Planar	20 mm	Water				T_{out} = 31.8 °C	η_{th} = 27.5%
				Graphite	Water	D = 50 nm	5-40 ppm	T_{out} = 40 - 43 °C	η_{th} = 59.0% - 72.0%
				Magnetite		D = 15 nm	5-40 ppm	T_{out} = 40 - 45 °C	η_{th} = 64.0% - 70.0%
				Ag		D = 20 nm	5-40 ppm	T_{out} = 34 - 35 °C	η_{th} = 35.0% - 38.0%
Lee *et al.* (2016) [133]	**Num./Exp.**	Planar	10 mm	Surface receiver				T_{out} = 120 °C	η_{th} = 75.4%
				MWCNT	Water	D = 20 nm	0.001-0.004 vol%	T_{out} = 60 - 100 °C	η_{th} = 75.0% - 87.2%
Vakili *et al.* (2016) [135]	**Experimental**	Planar	10 mm	Water (deionized)				-	η_{col} = 48.0% - 69.0%
				Graphene	Water	L = 2 µm	0.0005 wt%	-	η_{col} = 60.0% - 83.0%
							0.001 wt%	-	η_{col} = 64.0% - 89.0%
							0.005 wt%	-	η_{col} = 78.0% - 93.0%
Chen *et al.* (2017) [100]	**Experimental**	Tubular	40 mm	Water				T_{out} = 71 °C	η_{col} = 40% - 70%
				Graphene (G)	Water	-	0.02 wt%	T_{out} = 75.5 °C	η_{col} = 48% - 94%
				G-Oxide (GO)		L = 0.5 - 3 µm	0.02 wt%	T_{out} = 77 °C	η_{col} = 57% - 95%
				Reduced-GO		L = 0.5 - 3 µm	0.02 wt%	T_{out} = 82 °C	η_{col} = 65% - 96,93%
Gorji and Ranjbar (2017) [117]	**Numerical**	Planar	20 mm	Water				-	η_{th} = 27.5%
				Graphite	Water	D = 50 nm	39.8 ppm	-	η_{th} = 84.6%
				Magnetite		D = 15 nm	40 ppm	-	η_{th} = 94.3%
				Ag		D = 20 nm	38.6 ppm	-	η_{th} = 51.4%
Mehrali *et al.* (2018) [99]	**Experimental**	Planar	20 mm	Water (deionized)				-	η_{th} = 28%
				Reduced-Graphene Oxide	Water	-	10-100 ppm	ΔT = 18 °C	η_{th} = 54% - 62%
				Ag-rGO (0.15 g of Ag)		-	10-100 ppm	ΔT = 18 - 24 °C	η_{th} = 58% - 77%
				Ag-rGO (0.30 g of Ag)		-	10-100 ppm	ΔT = 18 - 24 °C	η_{th} = 53% - 78%
Siavashi *et al.* (2018) [148]	**Numerical**	Planar	5 - 20 mm	Water (deionized)				T_{out} = 21 - 28 °C	η_{col} = 15% - 30%
				Water (deionized) with absorbing plate at the bottom				T_{out} = 25 - 34 °C	η_{col} = 37% - 60%

				SWCNH	Water	D = 67 nm	5 - 40 ppm	T_{out} = 22 - 36 °C	η_{col} = 25% - 55%
				SWCNH with absorbing plate at the bottom				T_{out} = 23 - 35 °C	η_{col} = 35% - 59%
Bhalla *et al.* (2019) [146]	**Numerical**	Planar	6 - 10 mm	Amorphous carbon	Water	D < 50 nm	0.02 g/l	ΔT = 10 °C	η_{col} = 40%
							0.04 g/l	ΔT = 17 °C	η_{col} = 70%
							0.06 g/l	ΔT = 18.61 °C	η_{col} = 77%
Hooshmand *et al.* (2021) [147]	**Experimental**	Planar	20 mm	Water (deionized)				-	η_{col} = 35% - 65%
				Porous foam (SiC)	Water	-	-	-	η_{col} = 40% - 72%
				SiC	Water	D = 65 nm	1000 ppm	-	η_{col} = 48% - 78%
				SiC with porous foam (SiC)				-	η_{col} = 57% - 87%
Struchalin *et al.* (2021) [145]	**Num./Exp.**	Tubular	20 mm	Commercial FPC					η_{th} = 65% - 75%
				Commercial ETC					η_{th} = 74% - 77%
				MWCNT	Water	D = 49 - 72 nm L = 5 µm	0.0015 wt%		η_{th} = 45% - 70%
							0.0040 wt%		η_{th} = 60% - 87%
							0.0080 wt%		η_{th} = 75% - 94%
							0.01 wt%		η_{th} = 70% - 97%
							0.02 wt%		η_{th} = 58% - 81%

4.C.- Concentrating NDASC

The majority of studies on concentrating NDASC involve small or medium size PTC with tubular or planar linear receivers. As fluid temperatures are higher compared to non-concentrating NDASC, thermal oils are usually preferred over water. The main characteristics and performances of concentrating NDASC are summarized chronologically in **Table 5** and reviewed in the following paragraphs.

Statements made in the previous subsection regarding the influence of the type of nanoparticle, particle size and shape, particle volume fraction and fluid depths can be applied to concentrating NDASC. Carbon-based particles have shown better performances than metal and metal-oxide particles in concentrating collectors [88,151], as concluded in previous section by other authors [26,86,96,111,116]. To the authors knowledge, the scientific literature dedicated to hybrid [152,153] and plasmonic [154] nanofluids is very scarce, preventing any conclusion concerning their potential in concentrating NDASC to be established. The influence of the volume fraction and fluid depth has been evaluated and similar conclusions are achieved: there is an optimum volume fraction and fluid depth for which the collector efficiency reaches a maximum value (**Figure 9**) [89,155–158]. To our knowledge, the impact of the particle size and shape on the efficiency of concentrating NDASC has not been studied. Other important parameters, such as the nature of the base fluid or the working temperature, will be discussed in detail in the following paragraphs.

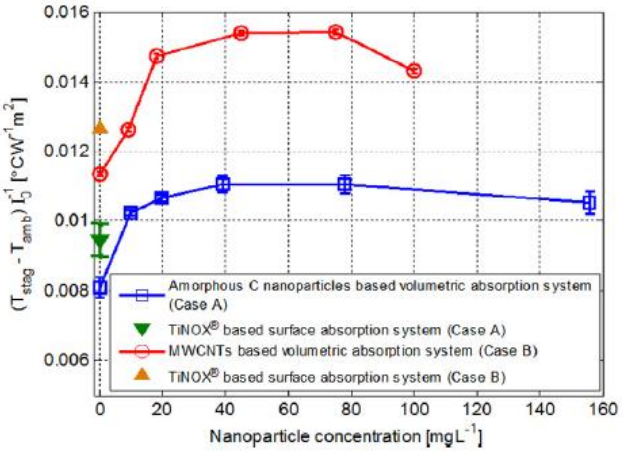

***Figure 9**: Normalized average stagnation temperature as a function of the nanoparticle concentration for two-carbon based NDASC (amorphous carbon and MWCNT) and two surface collectors. Reprinted from Ref.* [144] *with permission from Elsevier.*

Direct absorption parabolic trough collector (DAPTC) is by far the most commonly used concentrating technology in NDASC (see **Table 5**), thanks to its maturity (compared to LFC). Concentrating ratios (C) of DAPTC vary between 10 and 40 with relatively small receivers, around 20 mm in diameter in most cases, which can be classified as medium-size PTC (see **section 3**). O'Keeffe *et al.* [156] analyzed numerically the impact of C on the DAPTC efficiency and showed an increase in the collector efficiency until a threshold concentration value beyond which the efficiency reaches an asymptotic value due to increasing heat losses. Khullar *et al.* [159] concluded that the efficiency of the DAPTC decreases with the decrease of the incident radiation. From these works, it can be concluded that an optimum concentration ratio can be found for each system considering the fluid depths, which is related to the receiver size, and the size characteristics of the concentrator. Two studies used Fresnel lens as concentrating system, Singh *et al.* [158] and Li *et al.* [160,161], but no LFC or PDC have been used for concentrating NDASC.

Despite the domination of tubular receivers in the field of NDASC, planar receivers has also instigated some interest for NDASC [158,162,163]. Planar collectors offer the possibility of adding inner reflecting surfaces recovering the not-absorbed radiation by the fluid, which may lead to higher collector efficiencies as suggested by Singh *et al.* [158]. Otherwise, no-advantage of planar receivers over tubular receivers has been found. Khullar *et al.* [159] showed that the presence of vacuum layer surrounding the receiver led to reduced convective heat losses, translating into a 5 fold decrease in the heat losses and a 35% increase in the efficiency, relative to non-vacuum receivers. As outlined by several authors, vacuumed receivers only perform better than non-vacuumed receivers beyond a crucial working temperature [155,161]. When operating temperatures are below this crucial temperature, the lower convective heat losses do not compensate the lower optical efficiency of vacuumed receivers. Anti-emissivity coated receivers performance is also determined by a crucial operating temperature below which non-coated receivers are more efficient [156,157]. Therefore, vacuum receivers and anti-emissive coatings should be prioritized for concentrating NDASC operated at temperatures typically exceeding 150 °C.

The boiling temperature of water-based nanofluids limits their working range, the nanofluids being necessarily in liquid state to prevent particle deposition. Dugaria *et al.* [163] numerically showed outlet temperatures up to 143 °C using SWCNH at low concentrations (0.05 g/l) with a PTC and a planar receiver under pressure. Previous experimental study in similar conditions by the same authors demonstrated a significant particle deposition in the collector, lowering the collector efficiency by 18%. The stability issue was ascribed to an important degradation of the surfactant with increasing temperature [162]. Oil-based NDASC, however, can work at temperatures up to 250 °C (see **Table 5**) with Therminol VP-1 and WD synthetic oils being the most commonly used. Kasaeian *et al.* [89,155,164,165] studied ethylene glycol based nanofluids in a DAPTC; and proved the feasibility of such collector at temperatures up to 70 °C. Menbari *et al.* [166] compared a CuO/Al_2O_3 based nanofluid using water and a water-ethylene glycol mixture (50% each), and found slightly better efficiencies for the water based nanofluids. In general terms, water-based NDASC seem to perform better than oil and ethylene glycol based-nanofluids, but the temperature restriction may be an important constraint for practical applications like SHIP.

Compared to conventional concentrating surface collectors, concentrating NDASC have demonstrated higher efficiencies at temperatures up to ~150 °C (see **Table 5**) [89,144,152,159–163,167–169]. Xu *et al.* [168] and Chen *et al.* [169] outlined that there is a threshold temperature beyond which surface collectors outperform NDASC due to higher radiative losses compared to that of the selective absorbing surface. Anti-emissivity coating should be used in these cases as recommended by Li *et al.* [161] and O'Keeffe *et al.* [156]. Temperature should be carefully controlled as it is a critical parameter affecting the collector efficiency as well as the stability of nanoparticles (see section 5 for more information about the influence of temperature in the nanofluid stability) [162]. An innovative solution has been proposed by Heyhat *et al.* [170] adding porous metal foams inside the nanofluid-based volumetric receiver. They found higher thermal efficiencies (19% higher) than for a CuO-based concentrating NDASC. Singh *et al.* [158] studied experimentally the efficiency of a DAPTC using an 'used engine oil' containing carbon nanoparticles with a rectangular receiver with reflective lateral surfaces and obtained up to 60% thermal efficiencies. Novel designs may help improving the performance of current concentrating NDASC but their commercial viability should be further analyzed.

Table 5: Summary of concentrating NDASC studies in the literature

CONCENTRATING NDASC										
Authors (year) [ref]	Approach				Nanofluid				Results	
	Exp./Num.	Geometry	I_0 (W/m^2)	Fluid depth	Nanoparticles	Base Fluid	Size	Concentration	Temperature	Efficiency
Khullar *et al.* (2012) [159]	**Numerical**	PTC - Tube receiver	~ 60000	70 mm	SEGS LS-2 plant PTC collector (Syltherm 800)				ΔT = 16-240 °C	η_{th} = 70% - 73%
					Volumetric receiver (Therminol VP-1)				ΔT = 16-240 °C	η_{th} = 20% - 25%
					Al	Therminol VP-1	D = 5 nm	0.05 vol%	ΔT = 16-240 °C	η_{th} = 75% - 81%
									ΔT = 50-200 °C	η_{col} = 78% - 81%
Khullar *et al.* (2014) [144]	**Experimental**	Planar receiver	3000-5000	8 - 10 mm	Amorphous Carbon	Ethylene Glycol	D = 5 nm	10-150 mg/L	ΔT = ~50 °C	-
					MWCNT	Water	D = 31.5 nm L = 1.25 µm	10-150 mg/L	ΔT = ~47 °C	-
Li *et al.* (2015) [160]	**Experimental**	Fresnel lens - Tube receivers	4800	10 mm	Surface tube receiver (coated copper tube)				ΔT = 10-60 °C	η_{col} = 74% - 85%
					MWCNT	Water	D = 6-13 nm L = 2.5-20 µm	50 mg/L	ΔT = 10-60 °C	η_{col} = 54% - 73%
Xu *et al.* (2015) [168]	**Numerical**	PTC - Tube receiver	5152	45 mm	Surface receiver (WD synthetic oil)				ΔT = 125 °C	η_{col} = 42% - 52.5%
					CuO	WD synthetic oil	D = 200 nm	0.055 wt%	ΔT = 105 °C	η_{col} = 40% - 62%
Chen *et al.* (2016) [169]	**Numerical**	PTC - Tube receiver	4560	45 mm	Surface receiver (WD-350 synthetic oil)				-	η_{col} = 64.0%
					CuO	WD350 synth. oil	D = 200 nm	0.05 wt%	T_{in} = 40-110 °C	η_{col} = 63% - 70%
								0.06 wt%	T_{in} = 40-110 °C	η_{col} = 66% - 72%
								0.075 wt%	T_{in} = 40-110 °C	η_{col} = 65% - 72%
								0.1 wt%	T_{in} = 40-110 °C	η_{col} = 64% - 71%
Li *et al.* (2016) [161]	**Num./Exp.**	Fresnel lens - Tube pipes	3840	10 mm	Surface tube receiver - Therminol 55				T_{out} = 106-205 °C	η_{col} = 47% - 68%
					MWCNT	Therminol 55	-	50 mg/ml	T_{out} = 105-204 °C	η_{col} = 26% - 54%
Membari *et al.* (2016) [171]	**Num./Exp.**	PTC - Tube receiver	~ 44600	20 mm	CuO	Water	D = 100 nm	0.002 vol%	T_{out} = 28-36 °C	η_{th} = 28% - 33%
								0.004 vol%	T_{out} = 30-39 °C	η_{th} = 36% - 40%
								0.008 vol%	T_{out} = 31-42 °C	η_{th} = 41% - 49%
Toppin-Hector and Singh (2016) [88]	**Numerical**	PTC - Tube receiver	26000	5 - 25 mm	Graphene	Therminol VP-1	D = 5 nm	0.02 vol%	T_{out} = 127-267 °C	-
					Al		D = 5 nm	0.09 vol%	T_{out} = 127-267 °C	-
Bortolato *et al.* (2017) [162]	**Experimental**	PTC - Planar receiver	~ 37000	18 mm	Surface receiver (water)				-	η_{col} = ~80%
					SWCNT	Water	D = 2-5 nm L = 30-50 nm	0.02 g/L	-	η_{col} = 80% (3h exposure)
									-	η_{col} = 65% (8h exposure)
	Numerical		6531	26 mm	Volumetric receiver (Ethylene Glycol)				T_{out} = 44-48 °C	η_{th} = 52.2% - 59.5%

Kasaeian *et al.* (2017.a) [155]		PTC - Tube receiver			Silica (SiO_2)	Ethylene Glycol	D = 6-15 nm	0.2-0.4 vol%	T_{out} = 44-55 °C	η_{th} = 55.9% - 70.9%
					MWCNT	Ethylene Glycol	D = 4-10 nm	0.2-0.5 vol%	T_{out} = 50-61 °C	η_{th} = 61% - 80.7%
Kasaeian *et al.* (2017.b) [164]	**Experimental**	PTC - Tube receiver	7464-9330	24 mm	Volumetric receiver (Ethylene Glycol)				T_{out} = 48.8 °C	η_{th} = 55.8%
					Silica (SiO_2)	Ethylene Glycol	D = 15 nm L = 10 µm	0.1-0.2- 0.3 vol%	T_{out} = 51-57 °C	η_{th} = 58% - 60% - 64%
					MWCNT		D = 10 nm L = 100 µm	0.1-0.2-0.3 vol%	T_{out} = 55-65 °C	η_{th} = 61% - 65% - 73%
Membari *et al.* (2017) [166]	**Experimental**	PTC - Tube receiver	~ 42500	20 mm	Binary nanofluid: CuO + Al_2O_3	Water or a water/ethylene glycol mixture (50% each)	CuO: D < 100 nm Al_2O_3: D < 40 nm	0.008 vol% CuO 0.2 vol% Al_2O_3	T_{out} = 38-59 °C	η_{th} = 36% - 48% (water)
									T_{out} = 24-45 °C	η_{th} = 35% - 45% (mix)
								0.004 vol% CuO 0.1 vol% Al_2O_3	T_{out} = 30-46 °C	η_{th} = 31% - 39% (water)
									T_{out} = 31-50 °C	η_{th} = 29% - 37% (mix)
								0.002 vol% CuO 0.05 vol% Al_2O_3	T_{out} = 29-49 °C	η_{th} = 23% - 31% (water)
									T_{out} = 28-42 °C	η_{th} = 22% - 30% (mix)
Wang *et al.* (2017) [151]	**Experimental**	CPC - Tube receiver	-	-	Graphene	WD thermal oil	L = 0.5-2 µm	0.06 mg/ml	-	η_{col} = 80.0%
					Graphite		-	0.06 mg/ml	-	η_{col} = 72.0%
					CuO		-	0.06 mg/ml	-	η_{col} = 68.0%
Dugaria *et al.* (2018) [163]	**Numerical**	PTC - Planar receiver	38700	12 - 18 mm	Surface receiver (water)				-	η_{th} = 77% - 85%
					SWCNH	Water	-	0.006 g/l	T_{out} = 130 °C	η_{th} = 76% - 80.7%
								0.01 g/l	T_{out} = 132 °C	η_{th} = 81.8% - 84.2%
								0.02 - 0.05 g/l	T_{out} = 134-143 °C	η_{th} = 84.8% - 84.9%
O'Keeffe *et al.* (2018.a) [156]	**Numerical**	PTC - Tube receiver	1000-25000	16 mm	Volumetric receiver (Therminol VP-1)				-	η_{col} = 25.0%
					Al	Therminol VP-1	-	0.001 - 0.006 vol%	-	η_{col} = 71% - 80%
O'Keeffe *et al.* (2018.b) [157]	**Numerical**	PTC - Tube receiver	5000-20000	5 mm	Al	Therminol VP-1	-	0.001 vol%	-	η_{col} = ~25.0%
								0.006 vol%	-	η_{col} =~ 73% - 76%
								0.01 vol%	-	η_{col} =~ 75% - 78%
Kasaeian *et al.* (2019) [89]	**Numerical**	PTC - Tube receiver	7464-9330	26 mm	MWCNT	Ethylene Glycol	D = 4-10 nm	0.4 vol%	T_{out} = 56-65 °C	η_{th} = 68% - 79%
								0.5 vol%	T_{out} = 59-69 °C	η_{th} = 62.5% - 82.3%
								0.6 vol%	T_{out} = 62-72 °C	η_{th} = 76% - 82.3%
Heyhat *et al.* (2020) [170]	**Experimental**	PTC - Tube receiver	25500-28500	22 mm	Porous foam (CuO)	Water	-	-	-	η_{th} = 49.4%
					CuO	Water	D = 30 nm	0.01 - 0.1 vol%	-	η_{th} = 53.5% - 64.6%
					CuO with porous foam			0.01 - 0.1 vol%	-	η_{th} = 70% - 79.3%
	Experimental		~63000	15 mm	Water (deionized)				ΔT = 2.1 - 2.7 °C	η_{th} = 13.8% - 15.9%

Joseph *et al.* (2020) [154]		PTC - Tube receiver			SiO_2/Ag-CuO	Water	SiO_2/Ag: D = 300 nm CuO: D < 50 nm	SiO_2/Ag: 0.21 g/l CuO: 0.86 g/l	ΔT = 10.8 - 8.4 °C	η_{th} = 55% - 64.1%
Khalil *et al.* (2020) [152]	**Experimental**	PTC - Tube receiver	15000-19000	15 mm	Conventional PTC with Al_2O_3-CuO	Water	Al_2O_3: D < 100 nm CuO: D < 100 nm	0.11 - 0.55 vol%	ΔT = 4.5 - 6 °C	η_{th} = 26.6% - 45.4%
					Al_2O_3-CuO				ΔT = 4 - 6 °C	η_{th} = 30.6% - 58.4%
Ham *et al.* (2021) [167]	**Experimental**	CPC - Tube receivers	1015	18 mm	Surface receiver (water)				-	η_{th} = 42%
					Surface receiver (Fe_3O_4 nanofluid with 0.001-0.1 wt%)				-	η_{th} = 36% - 38%
					Fe_3O_4	Water	D = 6-15 nm	0.001 - 0.1 wt%	-	η_{th} = 42% - 50 %
Saray and Heyhat (2022) [153]	**Numerical**	PTC - Tube receiver	~28700	20 - 50 mm	Water (deionized)				-	η_{th} = 30% - 34%
					CuO	Water	-	0.1 - 0.05 wt%	-	η_{th} = 39% - 48%
					MWCNT		-	0.0015 wt%	-	η_{th} = 51% - 55%
					CuO-MWCNT		-	CuO: 0.1 - 0.05 wt% MWCNT: 0.0015 wt%	-	η_{th} = 60% - 66%

4.D.- Conclusion

Non-concentrating NDASC are able to enhance the performance of conventional planar collectors by 10-15%, while concentrating NDASC exhibit only minor improvements in comparison with conventional concentrating surface collectors. Carbon nanoparticles typically show slightly better performances than metal or metal-oxide nanoparticles in both non-concentrating and concentrating collectors. The choice of the base fluid does not significantly affect the thermal performance of the collector but is an important factor limiting the working temperature range in concentrating NDASC. The thermal conductivity is enhanced by the addition of nanoparticles but represents less than 4% of the absolute thermal efficiency increase [86,87], and therefore should not be considered as a crucial parameter for the optimization of DASC efficiency. Operating temperatures exceeding 150 °C have been proved to affect the nanofluid stability considerably due to an important surfactant degradation, and thus prevent NDASC from outperforming conventional surface collectors. In the light of these observations, NDASC applications should mainly be focused in low or medium temperature heat supply. As outlined in section 2, SHIP plants offer a promising application sector for medium-size solar collectors with numerous case studies and well documented commercialization strategies. The typical dimensions of the different families of medium-size solar collectors being consistent with the characteristic size of NDASC, the combination of these two technologies could thus provide a significant added value for SHIP applications over other competing technologies. To our knowledge, no studies addressed the integration of NDASC in SHIP applications, only few studies being dedicated to residential heating and cooling [135,172] or water desalination [173]. Future NDASC studies considering the working conditions of SHIP applications should be carried out to quantify the potential of concentrating NDASC in the industrial sector.

5. Challenges

Alagumalai *et al.* [174] identified, analyzed and quantified ten main barriers preventing nanofluid commercialization , and suggested a roadmap to overcome them. In the following, five main challenges are addressed.

5.A.- Stability of nanofluids

The long-term stability of nanofluids is a fundamental requirement for most of the practical applications and an important hurdle hindering nanofluid commercialization. Due to various forces (Van der Waals forces, electrostatic force, Brownian motion, etc…), nanoparticles are likely to agglomerate, causing sedimentation which alter the thermo-physical and optical properties of nanofluids, and may cause clogging of the hydraulic components. Some factors highly influencing the stability of nanofluids are: the dielectric constant of the base fluid, the zeta potential and the pH value of the nanofluid, the particle size and shape, and the particle volume fraction. The dielectric constant is directly proportional to the potential difference between two charged nanoparticles, which works as a barrier preventing particle agglomeration caused by Van der Waals forces [175]. Thus, base fluids with higher dielectric constant would offer more stable nanoparticle dispersions. The dielectric constant of water (78.5 at 20 °C) is higher than that of ethylene glycol or ethanol (24.6 at 20 °C), which makes water a better base fluid candidate [175,176]. Hordy *et al.* [177] analyzed the stability of plasma-functionalized MWCNT dispersed in various base fluids as a function of temperature and showed a high instability of the Therminol VP-1 nanofluid, while water and ethylene glycol based nanofluids showed a satisfying stability for 8 months.

The zeta potential indicates the degree of electrostatic repulsion between nanoparticles, with higher absolute values of the zeta potential indicating higher electrostatic repulsive forces. As an order

of magnitude, a nanoparticle dispersion is considered stable when the zeta potential is higher than 30 mV or lower than -30 mV [114,175,176,178,179] (**Figure 10**). The zeta potential, dependent of the particle material, decreases with the pH of the nanofluids. Consequently, low pH solutions (less than 6 [176,178]) exhibit a better stability than medium pH dispersions (**Figure 10**). If high pH values are reached, the zeta potential may drop below -30 mV, promoting the nanofluid stability [180,181,166]. However, very high (pH above 9) or very low (pH below 4) values may trigger an accelerated deterioration of the hydraulic equipment due to corrosion and restrict the possible nanofluid applications [114,179].

The stability of the nanofluid decreases with increasing particle size [114,176,182]. On the other hand, increasing the particle volume fraction induces higher Van der Waals attractive forces and therefore higher particle agglomeration [182]. This conclusion was achieved by several studies and suggests that low volume fraction nanofluids should be further investigated. Last, the working conditions of the collector have a critical influence on the stability of the dispersion. High temperatures induce high diffusion coefficients, likely to enhance the particle aggregation due to the high number of collisions [176]. Also, high temperatures have been proven to accelerate the surfactant degradation in nanofluids and thus affect the dispersion stability [114,162]. Deposition of nanoparticles is shown to be reduced in turbulent flow regime [145].

The method followed for synthesizing the nanofluid (which is either a one-step or a two-step method), is a key factor in the stability of nanofluids [114]. The one-step method allows a fine tuning of the particle size and shape, minimized particle agglomeration and, in turn, highly stable nanofluids. Unfortunately, the one-step method is only suitable for low quantities of nanofluid, and induce high production costs. The two-steps method is a cost-effective option adapted to large-scale production, but suffers from higher particle agglomeration which necessarily requires stabilization methods to be applied. Further information regarding preparation methods and supplementary stabilization techniques can be found in Mukherjee *et al.* [175] and Chakraborty and Panigrahi [176] reviews. New emerging synthesis techniques, such as the innovative method of Carbon Waters® for aqueous dispersions of exfoliated nanocarbons [183], are expected to improve the stability and to reduce the current production cost of nanofluids.

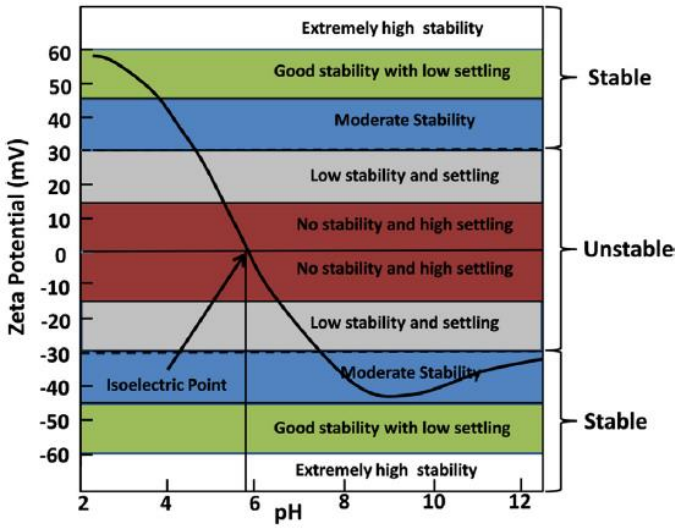

***Figure 10**: Scheme of the stability zones as a function of the zeta potential (mV) and the pH of the fluid. Reprinted from Ref.* [176] *with permission from Elsevier.*

5.B.- Toxicity and environmental impact

Due to their very small size, nanoparticles are able to enter living organisms, facilitating bacterial mutation, cell and protein degeneration and other harmful changes affecting living beings. Toxicological studies have demonstrated that the toxicity level increases for decreasing nanoparticle size [139,184]. The geometry and the chemical properties also affect the toxicity level of a given family of nanoparticles [185,186]. SWCNTs, tubular particles, were reported to induce higher pulmonary toxicity than spherical carbon black particles [184]. These particle show higher toxicity than quartz dust, that are known for causing serious lung diseases [187,188]. For metal nanoparticles, Schrand *et al.* [189] compared and ranked commonly used nanoparticles based on *in vitro testing*: Zn-based > Cu > Ag > Fe_3O_4 > Al_2O_3 > TiO_2. The toxicity level of nanofluids used in DASC is highly difficult to evaluate, since it is affected by many different factors (base fluid, particle, surfactants, stability, volume fraction, composition, uniformity, etc…). Further studies and experimental data on the toxicity of nanofluids are needed to determine the toxicity limit, the security measures, and the nano-wastes management in the future [27,109,174,190].

As outlined above, NDASC can achieve better efficiencies than conventional collectors, which may generate important energy savings and CO2 emissions drop. Otanicar *et al.* [191] evaluated the CO2 emissions saving associated with a planar NDASC over a 15 year lifetime, and estimated that respectively 740 kg and 23 000 kg CO2 emissions could be saved in comparison with a conventional FPC and a traditional water heater, respectively. The use of a CuO2 water-based nanofluid as HTF on a conventional FPC was shown to offset CO2 emissions by 175 kg in comparison with water. Gupta *et al.* [192] evaluated the energy savings associated with the substitution of 50% of the conventional collectors currently installed by NDASC, and concluded that the corresponding energy reduction would represent 857.5 millions of MJ/year. However, at the end of their life cycle, NDASC generate nano-wastes, whose management still needs to be improved and standardized (see Part *et al.* [193] for further information about nano-waste characterization and separation techniques). In the Younis *et al.* [194] book section, the nano-waste risk profiles of different nanomaterials are presented and classified, allowing the reader to identify and estimate the precautions for managing nano-waste.

5.C.- Pumping power

The addition of nanoparticles induces an increase in the viscosity of the base fluid, which entails higher pumping power and, thus, higher operational costs [114]. The viscosity of the base fluid was shown to be only slightly affected by the incorporation of graphene nanoplatelets [108] and nitrogen-doped graphene [107] for low quantities of nanoparticles (less than 0.1 wt%). The influence of the MWCNT shape on the nanofluid viscosity was scrutinized by Omrani *et al.* [195], who demonstrated that high aspect ratio particles induce less viscosity growth. Chiam *et al.* [196] quantified dependence of viscosity on the volume fraction of nanoparticles and underlined the significant viscosity growth expected for large volume fractions. However, the range of volume fraction investigated by these authors exceeds the typical particle concentration commonly associated with NDASC (which is typically comprised between 0.001 and 0.1 vol% (see **Table 4** and **5**)) and thus expected viscosity enhancements are low. Nevertheless, due to the positive correlation between viscosity and nanoparticle concentration, nanofluids characterized by lower particle volume fraction should offer pore promising properties and should thus be privileged.

5.D.- Erosion and corrosion of components

Erosion and corrosion associated with the incorporation of nanoparticles constitute a serious hurdle which must necessarily be tackled. Celata *et al.* [197] and Fotowat *et al.* [198] studied the corrosion of both metal and metal-oxides nanoparticles and observed that stainless steel pipes were

not affected, unlike aluminum and copper pipes, which both show significant degradations. Stainless steel components are therefore recommended for the hydraulic circuit of the NDASC installation. The influence of the type of nanoparticles was also investigated by several authors, who demonstrated lower corrosion for carbon-based nanofluids in comparison with metal or oxide based nanofluids [113,199,200].

5.E.- Production costs

The cost of selective nanoparticles together with the synthesis costs leads to nanofluids costs that are much higher than those of conventional HTF in surface collectors (water or thermal oils). The economic analysis of Wciślik [201] and Alirezaie *et al.* [202] underlines the low cost of metal-oxides nanoparticles (TiO_2, Al_2O_3, CuO or SiO_2) in comparison with metal particles (Ag, Al, Cu or Au), which are typically 10 times more expensive. Carbon-based nanotubes (single or double walled) are typically 10 times more expensive than metal nanoparticles, and 100 times more expensive than metal-oxides [202]. The prices of a given nanofluid is more subtle to quantify, because of the influence of the synthesis method as well as the cost calculation scenario followed [83,191,201,202]. As an order of magnitude, nanofluid cost with volume fractions of 0.04-0.1 are between 2-10 US$/L for metal-oxides, 100-500 US$/L for metals, and 300-1000 US$/L for carbon nanotubes [201,202]. Despite their lower efficiency in comparison with carbon-based NDASC, metal-oxide base NDASC are more cost-effective and thus show higher potential for rapid commercialization. Nanofluid prices are expected to decrease in the following years thanks to new synthesis techniques, however the increase of nanomaterial demand for numerous novel nanotechnology could offset these trends and prevent the rapid commercialization of NDASC.

6. Discussion and perspectives

The present work provides an overview of the application of solar energy for industrial processes involving low and medium temperature operation; the current solar thermal technologies used are exposed, and the latest progress on nanofluid-based direct absorption solar collectors (NDASC) are discussed. Important conclusions obtained from the literature review are summarized hereafter.

- Solar thermal collectors have huge potential in the industrial sector, particularly in the food sector, in countries with good solar resource (>1700 kWh/m² yearly total global horizontal irradiation). For less irradiated countries, governmental and international incentives for SHIP plants are required to replace progressively conventional carbon-based energy sources during a transition period, as previously done for photovoltaic (PV).
- The majority of SHIP installations require heat temperatures between 60 °C and 150 °C. Concentrating collectors, mainly PTC, show improved performance over planar collectors in this temperature range. Since, PTC valorize the direct solar irradiation only, yearly energy production must be simulated for choosing the best technology between concentrating and non-concentrating collectors for each application, in particular above 100°C.
- Among the different technologies discussed in section 3, PTC and LFC are the most promising options for SHIP applications, allowing the integration of a nanofluid-based volumetric receiver.
- The performance of NDASC is highly affected by the fluid temperature, which influences the nanofluid stability and increases heat losses with the environment. The nanofluid stability in medium temperature NDASC (i.e. 100-400 °C) needs to be further studied to better understand the temperature limitations. Heat losses may be reduced with vacuumed receivers and low-emissivity coated glass envelopes [156].

- NDASC optimal working conditions and heat demand of SHIP installations are close, which presents the industrial sector as a potential application sector for NDASC. Nevertheless, performance and viability need to be thoughtfully studied.

Further research involving outdoor experimental collectors is needed to carefully evaluate the performance and feasibility of NDASC in real working conditions and analyze the effect of nanoparticle size and shape. Carbon nanoparticles are particularly promising for solar applications, their performance being even higher than those of metal or oxides nanofluids [89,96,116,151,155,164,165]. Further research is needed on the technical-economic optimization of volumetric receivers depending on the working temperature range, focusing on low emissivity coatings for inner glass envelope with solar transmittance greater than 90%. Finally, performance and economic studies should be initiated to quantify the potential of NDASC for SHIP applications, as well as residential heating and cooling. The steps to follow towards the development of a NDASC from the laboratory scale to a commercial collector for process heat applications are resumed in **Figure 11**. Another application of interest which should be investigated is hybrid PVT systems that use nanofluids as optical filters to produce both electricity and process heat [203–226]. In this latter domain the variation of optical properties with wavelength is a key parameter that governs the overall efficiency of the hybrid converter. Photochemistry is a promising application sector for nanofluids as well.

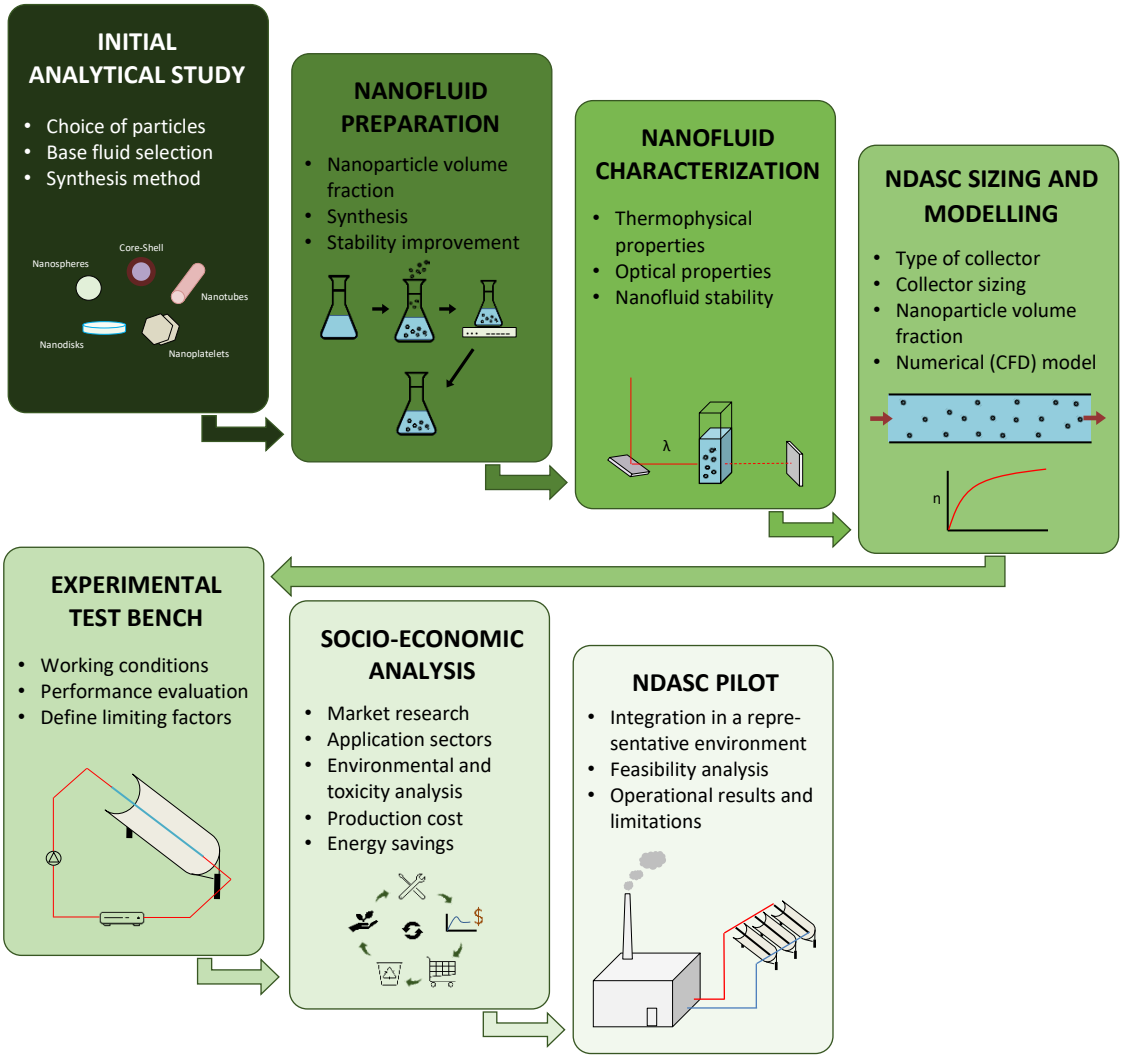

***Figure 11**: Steps for future NDASC commercialization towards SHIP applications.*

7. Acknowledgements

This work was supported by the French “Investments for the future” ("Investissements d'Avenir") program managed by the National Agency for Research (ANR) under contract ANR-10-LABX-22-01 (labex SOLSTICE).

8. References

[1] Otanicar TP, Phelan PE, Prasher RS, Rosengarten G, Taylor RA. Nanofluid-based direct absorption solar collector. Journal of Renewable and Sustainable Energy 2010;2:033102. https://doi.org/10.1063/1.3429737.

[2] IEA SHC. Technology Roadmap - Solar Heating and Cooling. Paris, France: International Energy Agency (IEA); 2012.

[3] Brunner, Christoph. Webinar: Cheaper than electrification: How solar heat will replace oil and gas in the EU industrial sector - Solar process heat and it's role in a future renewable energy supply. 2021.

[4] Weiss W, Spörk-Dür M. Solar Heat Worldwide - Global Market Development and Trends in 2020 & Detailed Market Data 2019. Gleisdorf, Austria: AEE INTEC and SHC; 2021.

[5] Weiss W, Rommel M. Process heat collectors - State of the art within Task 33/IV. Gleisdorf, Austria: IEA SHC-Task 33 and SolarPACES-Task IV; 2008.

[6] Tong Y, Kim J, Cho H. Effects of thermal performance of enclosed-type evacuated U-tube solar collector with multi-walled carbon nanotube/water nanofluid. Renewable Energy 2015;83:463–73. https://doi.org/10.1016/j.renene.2015.04.042.

[7] Sabiha MA, Saidur R, Hassani S, Said Z, Mekhilef S. Energy performance of an evacuated tube solar collector using single walled carbon nanotubes nanofluids. Energy Conversion and Management 2015;105:1377–88. https://doi.org/10.1016/j.enconman.2015.09.009.

[8] Verma SK, Tiwari AK, Chauhan DS. Experimental evaluation of flat plate solar collector using nanofluids. Energy Conversion and Management 2017;134:103–15. https://doi.org/10.1016/j.enconman.2016.12.037.

[9] Zayed ME, Zhao J, Du Y, Kabeel AE, Shalaby SM. Factors affecting the thermal performance of the flat plate solar collector using nanofluids: A review. Solar Energy 2019;182:382–96. https://doi.org/10.1016/j.solener.2019.02.054.

[10] Bellos E, Tzivanidis C. Thermal efficiency enhancement of nanofluid-based parabolic trough collectors. J Therm Anal Calorim 2019;135:597–608. https://doi.org/10.1007/s10973-018-7056-7.

[11] Minardi JE, Chuang HN. Performance of a "black" liquid flat-plate solar collector. Solar Energy 1975;17:179–83. https://doi.org/10.1016/0038-092X(75)90057-2.

[12] Tyagi H, Phelan P, Prasher R. Predicted Efficiency of a Low-Temperature Nanofluid-Based Direct Absorption Solar Collector. Journal of Solar Energy Engineering 2009;131. https://doi.org/10.1115/1.3197562.

[13] Otanicar TP, Phelan PE, Prasher RS, Rosengarten G, Taylor RA. Nanofluid-based direct absorption solar collector. Journal of Renewable and Sustainable Energy 2010;2:033102. https://doi.org/10.1063/1.3429737.

[14] Phelan P, Otanicar T, Taylor R, Tyagi H. Trends and Opportunities in Direct-Absorption Solar Thermal Collectors. Journal of Thermal Science and Engineering Applications 2013;5:021003. https://doi.org/10.1115/1.4023930.

[15] Mahian O, Kianifar A, Kalogirou SA, Pop I, Wongwises S. A review of the applications of nanofluids in solar energy. International Journal of Heat and Mass Transfer 2013;57:582–94. https://doi.org/10.1016/j.ijheatmasstransfer.2012.10.037.

[16] Nagarajan PK, Subramani J, Suyambazhahan S, Sathyamurthy R. Nanofluids for Solar Collector Applications: A Review. Energy Procedia 2014;61:2416–34. https://doi.org/10.1016/j.egypro.2014.12.017.

[17] Kasaeian A, Eshghi AT, Sameti M. A review on the applications of nanofluids in solar energy systems. Renewable and Sustainable Energy Reviews 2015;43:584–98. https://doi.org/10.1016/j.rser.2014.11.020.

[18] Verma S kumar, Tiwari AK. Application of Nanoparticles in Solar collectors: A Review. Materials Today: Proceedings 2015;2:3638–47. https://doi.org/10.1016/j.matpr.2015.07.121.

[19] Hussein AK. Applications of nanotechnology to improve the performance of solar collectors – Recent advances and overview. Renewable and Sustainable Energy Reviews 2016;62:767–92. https://doi.org/10.1016/j.rser.2016.04.050.
[20] Elsheikh AH, Sharshir SW, Mostafa ME, Essa FA, Ahmed Ali MK. Applications of nanofluids in solar energy: A review of recent advances. Renewable and Sustainable Energy Reviews 2018;82:3483–502. https://doi.org/10.1016/j.rser.2017.10.108.
[21] Khanafer K, Vafai K. A review on the applications of nanofluids in solar energy field. Renewable Energy 2018;123:398–406. https://doi.org/10.1016/j.renene.2018.01.097.
[22] Farhana K, Kadirgama K, Rahman MM, Ramasamy D, Noor MM, Najafi G, et al. Improvement in the performance of solar collectors with nanofluids — A state-of-the-art review. Nano-Structures & Nano-Objects 2019;18:100276. https://doi.org/10.1016/j.nanoso.2019.100276.
[23] Said Z, Hachicha AA, Aberoumand S, Yousef BAA, Sayed ET, Bellos E. Recent advances on nanofluids for low to medium temperature solar collectors: energy, exergy, economic analysis and environmental impact. Progress in Energy and Combustion Science 2021;84:100898. https://doi.org/10.1016/j.pecs.2020.100898.
[24] Hamzat AK, Omisanya MI, Sahin AZ, Ropo Oyetunji O, Abolade Olaitan N. Application of nanofluid in solar energy harvesting devices: A comprehensive review. Energy Conversion and Management 2022;266:115790. https://doi.org/10.1016/j.enconman.2022.115790.
[25] Raj P, Subudhi S. A review of studies using nanofluids in flat-plate and direct absorption solar collectors. Renewable and Sustainable Energy Reviews 2018;84:54–74. https://doi.org/10.1016/j.rser.2017.10.012.
[26] Trong Tam N, Viet Phuong N, Hong Khoi P, Ngoc Minh P, Afrand M, Van Trinh P, et al. Carbon Nanomaterial-Based Nanofluids for Direct Thermal Solar Absorption. Nanomaterials 2020;10:1199. https://doi.org/10.3390/nano10061199.
[27] Kumar S, Chander N, Gupta VK, Kukreja R. Progress, challenges and future prospects of plasmonic nanofluid based direct absorption solar collectors – A state-of-the-art review. Solar Energy 2021;227:365–425. https://doi.org/10.1016/j.solener.2021.09.008.
[28] Rasih RA, Sidik NAC, Samion S. Recent progress on concentrating direct absorption solar collector using nanofluids: A review. J Therm Anal Calorim 2019;137:903–22. https://doi.org/10.1007/s10973-018-7964-6.
[29] Rasih RA, Sidik NAC, Samion S. Numerical Investigation of Direct Absorption Solar Collector using Nanofluids: A Review. IOP Conf Ser: Mater Sci Eng 2019;469:012059. https://doi.org/10.1088/1757-899X/469/1/012059.
[30] Fu B, Zhang J, Chen H, Guo H, Song C, Shang W, et al. Optical nanofluids for direct absorption-based solar-thermal energy harvesting at medium-to-high temperatures. Current Opinion in Chemical Engineering 2019;25:51–6. https://doi.org/10.1016/j.coche.2019.07.002.
[31] Karami M, Bozorgi M, Delfani S. Effect of design and operating parameters on thermal performance of low-temperature direct absorption solar collectors: a review. J Therm Anal Calorim 2021;146:993–1013. https://doi.org/10.1007/s10973-020-10043-z.
[32] Gorji TB, Ranjbar AA. A review on optical properties and application of nanofluids in direct absorption solar collectors (DASCs). Renewable and Sustainable Energy Reviews 2017;72:10–32. https://doi.org/10.1016/j.rser.2017.01.015.
[33] Chamsa-ard W, Brundavanam S, Fung CC, Fawcett D, Poinern G. Nanofluid Types, Their Synthesis, Properties and Incorporation in Direct Solar Thermal Collectors: A Review. Nanomaterials 2017;7:131. https://doi.org/10.3390/nano7060131.
[34] Weiss W. Meeting: Solar Heat for Industry - Potential of Solar Process Heat - AEE INTEC 2013.
[35] Solar Payback. Solar Heat for Industry - South Africa. Germany: Solar Payback; 2019.
[36] Farjana SH, Huda N, Mahmud MAP, Saidur R. Solar process heat in industrial systems – A global review. Renewable and Sustainable Energy Reviews 2018;82:2270–86. https://doi.org/10.1016/j.rser.2017.08.065.
[37] IEA, IRENA. Solar Heat for Industrial Processes - Technology Brief. IEA-ETSAP and IRENA Technology Brief; 2015.

[38] IEA Task 49/IV. Solar Thermal Plants Database 2021. http://ship-plants.info/solar-thermal-plants (accessed October 1, 2021).
[39] Häberle A. Concentrating solar technologies for industrial process heat and cooling. Concentrating Solar Power Technology, Elsevier; 2012, p. 602–19. https://doi.org/10.1533/9780857096173.3.602.
[40] Thermal Cooling Technology (TCT). True Solar Power n.d. https://www.truesolarpower.es/ (accessed January 14, 2022).
[41] Ktistis PK, Agathokleous RA, Kalogirou SA. Experimental performance of a parabolic trough collector system for an industrial process heat application. Energy 2021;215:119288. https://doi.org/10.1016/j.energy.2020.119288.
[42] Goswami RP. An optimistic growth of CSTs in India. SUN FOCUS 2017;4:6–7.
[43] IEA SHC. Solar Heating & Cooling Programme - International Energy Agency. Who We Are n.d. https://iea-shc.org/who-we-are (accessed April 16, 2021).
[44] IEA SHC, SolarPACES. Task 64/IV - Solar Process Heat 5th Experts Meeting - Presentation of the Subtasks 2021.
[45] Solar Heat Europe. Missions & Goals n.d. http://solarheateurope.eu/solar-heat-europe/solar-heat-europe-missions-values/ (accessed April 16, 2021).
[46] Alghoul MA, Sulaiman MY, Azmi BZ, Wahab MAbd. Review of materials for solar thermal collectors. Anti-Corrosion Meth & Material 2005;52:199–206. https://doi.org/10.1108/00035590510603210.
[47] Weiss W, Spörk-Dür M. Solar Heat Worldwide - Global Market Development and Trends in 2019 & Detailed Market Data 2018. Gleisdorf, Austria: AEE INTEC and SHC; 2020.
[48] Kalogirou SA. Solar thermal collectors and applications. Progress in Energy and Combustion Science 2004;30:231–95. https://doi.org/10.1016/j.pecs.2004.02.001.
[49] Solar Rating & Certification Corporation. Rating Summary page n.d. https://secure.solar-rating.org/Certification/Ratings/RatingsSummaryPage (accessed January 12, 2022).
[50] Williamson T, Davis P. Comparison of Performance for Evacuated Tube and Flat Plate Solar Collectors for Domestic Hot Water Applications in Northerly Climates. 3RD EUROPEAN SOLAR THERMAL ENERGY CONFERENCE, 2007, p. 378.
[51] Solar Rating & Certification Corporation (ICC-SRCC). OG-100 Certified Solar Thermal Collector Directory. Rating Summary Page n.d. https://secure.solar-rating.org/Certification/Ratings/RatingsSummaryPage.aspx?type=1 (accessed March 10, 2022).
[52] Falcoz Q. Class Lecture at the Université de Perpignan Via Domitia: Concentrated Solar Power - Part 1 2019.
[53] Günther M, Eickhoff M, Khalil T, Meyer-Grünefeldt M. Linear Fresnel Technology. Advanced CSP Teaching Materials, Enermena 2006:43.
[54] Fernández-García A, Zarza E, Valenzuela L, Pérez M. Parabolic-trough solar collectors and their applications. Renewable and Sustainable Energy Reviews 2010;14:1695–721. https://doi.org/10.1016/j.rser.2010.03.012.
[55] Abbas R, Muñoz-Antón J, Valdés M, Martínez-Val JM. High concentration linear Fresnel reflectors. Energy Conversion and Management 2013;72:60–8. https://doi.org/10.1016/j.enconman.2013.01.039.
[56] Bernhard R, Laabs H-J, de Lalaing J, Eck M, Eickhoff M, Pottler K, et al. LINEAR FRESNEL COLLECTOR DEMONSTRATION ON THE PSA PART I – DESIGN; CONSTRUCTION AND QUALITY CONTROL n.d.:10.
[57] Zhu G, Wendelin T, Wagner MJ, Kutscher C. History, current state, and future of linear Fresnel concentrating solar collectors. Solar Energy 2014;103:639–52. https://doi.org/10.1016/j.solener.2013.05.021.
[58] PROMES CNRS. Concentrateurs solaires n.d. https://www.promes.cnrs.fr/index.php?page=concentrateurs-solaires#prettyPhoto (accessed May 11, 2021).

[59] Pino FJ, Caro R, Rosa F, Guerra J. Experimental validation of an optical and thermal model of a linear Fresnel collector system. Applied Thermal Engineering 2013;50:1463–71. https://doi.org/10.1016/j.applthermaleng.2011.12.020.
[60] IT Power India. Material and Component Specifications Fresnel Reflector Based Dish with Moving Focus (ARUN). New Delhi, India: Ministry of New and Renewable Energy Government of India; 2015.
[61] Kumar A, Prakash O, Kaviti AK. A comprehensive review of Scheffler solar collector. Renewable and Sustainable Energy Reviews 2017;77:890–8. https://doi.org/10.1016/j.rser.2017.03.044.
[62] IT Power India. Material and component specifications: fixed focus automatically tracked elliptical dish (Scheffler). New Delhi, India: Ministry of New and Renewable Energy Government of India; 2015.
[63] Wu S-Y, Xiao L, Cao Y, Li Y-R. Convection heat loss from cavity receiver in parabolic dish solar thermal power system: A review. Solar Energy 2010;84:1342–55. https://doi.org/10.1016/j.solener.2010.04.008.
[64] Abhishek K, Udawant R. Highlights of CST field projects supported under UNDP CSHP. SUN FOCUS 2017;4:12–5.
[65] Pulfer J-C, Ingeniería C, López RM. SMALL MARMALADE FACTORY IN ARGENTINA WORKING WITH SCHEFFLER TYPE INDUSTRIAL COOKER, Sacramento, CA, USA: Solar Cookers International; 2006, p. 4.
[66] Müller C, EcoAndina F, Arias C. International Solar Food Processing Conference - Solar community bakeries on the Argentinean Altiplano, 2009.
[67] EMS Focus. Concentrateur Solaris n.d. https://www.emsfocus.fr/concentrateur-solaris.html (accessed January 13, 2022).
[68] Soliterm group. Parabolic Trough Collectors. Soliterm - Technology n.d. https://solitermgroup.com/technology/ (accessed January 13, 2022).
[69] Absolicon. T160 Solar collector - Data Sheet n.d. https://www.absolicon.com/wp-content/uploads/2021/06/05_T160-Solar-Collector_Datasheet.pdf (accessed January 13, 2022).
[70] Helioclim. Absorbeurs solaires des capteurs Heliolight 4800. Technologies n.d. http://www.helioclim.fr/technologies/ (accessed January 13, 2022).
[71] Rioglass Solar. Receiver Tubes for Linear CSP Applications. HCE Tubes n.d. https://www.rioglass.com/our-products/hce-tubes.html (accessed January 13, 2022).
[72] Inventive Power. Power Trough 110®. Technology n.d. https://inventivepower.com.mx/english/power-trough-110/ (accessed January 13, 2022).
[73] Inventive Power. Power Trough 250®. Technology n.d. https://inventivepower.com.mx/english/power-trough-250/ (accessed January 13, 2022).
[74] NEP Solar Pty. Ltd. Technical Data for the PolyTrough 1200. Zurich, Switzerland: n.d.
[75] Industrial Solar GmbH. Fresnel Collector LF-11 n.d. https://www.industrial-solar.de/en/technologies/fresnel-collector/ (accessed January 13, 2022).
[76] Chromasun Inc. The Chromasun Micro-Concentrator (MCT) panel n.d. http://www.chromasun.com/MCT.html (accessed January 13, 2022).
[77] RioGlass®. Sun2Heat Solutions n.d. https://www.rioglass.com/our-products/sun2heat-solutions (accessed January 13, 2022).
[78] Del Prado, Pablo, IEA SHC. Task 64/IV - Solar Process Heat 5th Experts Meeting - Project presentation: Rioglass with Sun2Heat 2021.
[79] Solatom. FLT 20 - Linear Fresnel Solar Collector n.d. https://www.solatom.com/index_en.html (accessed January 4, 2022).
[80] Soltigua. FLT - The ideal solution for cooling and process heat n.d. https://www.soltigua.com/flt-introducion/ (accessed January 13, 2022).
[81] Spoladore M, Camacho EF, Valcher ME. Distributed Parameters Dynamic Model of a Solar Fresnel Collector Field. IFAC Proceedings Volumes 2011;44:14784–9. https://doi.org/10.3182/20110828-6-IT-1002.02992.

[82] Gharbi NE, Derbal H, Bouaichaoui S, Said N. A comparative study between parabolic trough collector and linear Fresnel reflector technologies. Energy Procedia 2011;6:565–72. https://doi.org/10.1016/j.egypro.2011.05.065.
[83] Ladjevardi SM, Asnaghi A, Izadkhast PS, Kashani AH. Applicability of graphite nanofluids in direct solar energy absorption. Solar Energy 2013;94:327–34. https://doi.org/10.1016/j.solener.2013.05.012.
[84] Cregan V, Myers TG. Modelling the efficiency of a nanofluid direct absorption solar collector. International Journal of Heat and Mass Transfer 2015;90:505–14. https://doi.org/10.1016/j.ijheatmasstransfer.2015.06.055.
[85] Gorji TB, Ranjbar AA. Geometry optimization of a nanofluid-based direct absorption solar collector using response surface methodology. Solar Energy 2015;122:314–25. https://doi.org/10.1016/j.solener.2015.09.007.
[86] Gorji TB, Ranjbar AA. A numerical and experimental investigation on the performance of a low-flux direct absorption solar collector (DASC) using graphite, magnetite and silver nanofluids. Solar Energy 2016;135:493–505. https://doi.org/10.1016/j.solener.2016.06.023.
[87] Delfani S, Karami M, Behabadi MAA-. Performance characteristics of a residential-type direct absorption solar collector using MWCNT nanofluid. Renewable Energy 2016;87:754–64. https://doi.org/10.1016/j.renene.2015.11.004.
[88] Toppin-Hector A, Singh H. Development of a nano-heat transfer fluid carrying direct absorbing receiver for concentrating solar collectors. Int J Low-Carbon Tech 2016;11:199–204. https://doi.org/10.1093/ijlct/ctt072.
[89] Kasaeian A, Daneshazarian R, Pourfayaz F, Babaei S, Sheikhpour M, Nakhjavani S. Evaluation of MWCNT/ethylene glycol nanofluid flow in a parabolic trough collector with glass-glass absorber tube. HFF 2019;30:176–205. https://doi.org/10.1108/HFF-11-2018-0693.
[90] Saidur R, Meng TC, Said Z, Hasanuzzaman M, Kamyar A. Evaluation of the effect of nanofluid-based absorbers on direct solar collector. International Journal of Heat and Mass Transfer 2012;55:5899–907. https://doi.org/10.1016/j.ijheatmasstransfer.2012.05.087.
[91] Lee S-H, Jang SP. Extinction coefficient of aqueous nanofluids containing multi-walled carbon nanotubes. International Journal of Heat and Mass Transfer 2013;67:930–5. https://doi.org/10.1016/j.ijheatmasstransfer.2013.08.094.
[92] Song D, Wang Y, Jing D, Geng J. Investigation and prediction of optical properties of alumina nanofluids with different aggregation properties. International Journal of Heat and Mass Transfer 2016;96:430–7. https://doi.org/10.1016/j.ijheatmasstransfer.2016.01.049.
[93] Potenza M, Milanese M, Colangelo G, de Risi A. Experimental investigation of transparent parabolic trough collector based on gas-phase nanofluid. Applied Energy 2017;203:560–70. https://doi.org/10.1016/j.apenergy.2017.06.075.
[94] Freedman JP, Wang H, Prasher RS. Analysis of Nanofluid-Based Parabolic Trough Collectors for Solar Thermal Applications. Journal of Solar Energy Engineering 2018;140:051008. https://doi.org/10.1115/1.4039988.
[95] Lee BJ, Park K, Walsh T, Xu L. Radiative Heat Transfer Analysis in Plasmonic Nanofluids for Direct Solar Thermal Absorption. Journal of Solar Energy Engineering 2012;134:021009. https://doi.org/10.1115/1.4005756.
[96] Luo Z, Wang C, Wei W, Xiao G, Ni M. Performance improvement of a nanofluid solar collector based on direct absorption collection (DAC) concepts. International Journal of Heat and Mass Transfer 2014;75:262–71. https://doi.org/10.1016/j.ijheatmasstransfer.2014.03.072.
[97] Jeon J, Park S, Lee BJ. Optical property of blended plasmonic nanofluid based on gold nanorods. Opt Express, OE 2014;22:A1101–11. https://doi.org/10.1364/OE.22.0A1101.
[98] Taylor RA, Phelan PE, Otanicar TP, Adrian R, Prasher R. Nanofluid optical property characterization: towards efficient direct absorption solar collectors. Nanoscale Res Lett 2011;6:225. https://doi.org/10.1186/1556-276X-6-225.

[99] Mehrali M, Ghatkesar MK, Pecnik R. Full-spectrum volumetric solar thermal conversion via graphene/silver hybrid plasmonic nanofluids. Applied Energy 2018;224:103–15. https://doi.org/10.1016/j.apenergy.2018.04.065.
[100] Chen L, Liu J, Fang X, Zhang Z. Reduced graphene oxide dispersed nanofluids with improved photo-thermal conversion performance for direct absorption solar collectors. Solar Energy Materials and Solar Cells 2017;163:125–33. https://doi.org/10.1016/j.solmat.2017.01.024.
[101] Nair RR, Blake P, Grigorenko AN, Novoselov KS, Booth TJ, Stauber T, et al. Fine Structure Constant Defines Visual Transparency of Graphene. Science 2008;320:1308–1308. https://doi.org/10.1126/science.1156965.
[102] Jyothirmayee Aravind SS, Ramaprabhu S. Surfactant free graphene nanosheets based nanofluids by in-situ reduction of alkaline graphite oxide suspensions. Journal of Applied Physics 2011;110:124326. https://doi.org/10.1063/1.3671613.
[103] Sani E, Mercatelli L, Barison S, Pagura C, Agresti F, Colla L, et al. Potential of carbon nanohorn-based suspensions for solar thermal collectors. Solar Energy Materials and Solar Cells 2011;95:2994–3000. https://doi.org/10.1016/j.solmat.2011.06.011.
[104] Sen Gupta S, Manoj Siva V, Krishnan S, Sreeprasad TS, Singh PK, Pradeep T, et al. Thermal conductivity enhancement of nanofluids containing graphene nanosheets. Journal of Applied Physics 2011;110:084302. https://doi.org/10.1063/1.3650456.
[105] Yu W, Xie H, Wang X, Wang X. Significant thermal conductivity enhancement for nanofluids containing graphene nanosheets. Physics Letters A 2011;375:1323–8. https://doi.org/10.1016/j.physleta.2011.01.040.
[106] Karami M, Akhavan Bahabadi MA, Delfani S, Ghozatloo A. A new application of carbon nanotubes nanofluid as working fluid of low-temperature direct absorption solar collector. Solar Energy Materials and Solar Cells 2014;121:114–8. https://doi.org/10.1016/j.solmat.2013.11.004.
[107] Mehrali M, Sadeghinezhad E, Tahan Latibari S, Mehrali M, Togun H, Zubir MNM, et al. Preparation, characterization, viscosity, and thermal conductivity of nitrogen-doped graphene aqueous nanofluids. J Mater Sci 2014;49:7156–71. https://doi.org/10.1007/s10853-014-8424-8.
[108] Mehrali M, Sadeghinezhad E, Latibari ST, Kazi SN, Mehrali M, Zubir MNBM, et al. Investigation of thermal conductivity and rheological properties of nanofluids containing graphene nanoplatelets. Nanoscale Res Lett 2014;9:15. https://doi.org/10.1186/1556-276X-9-15.
[109] Krajnik P, Pusavec F, Rashid A. Nanofluids: Properties, Applications and Sustainability Aspects in Materials Processing Technologies. In: Seliger G, Khraisheh MMK, Jawahir IS, editors. Advances in Sustainable Manufacturing, Berlin, Heidelberg: Springer Berlin Heidelberg; 2011, p. 107–13. https://doi.org/10.1007/978-3-642-20183-7_16.
[110] Ahmad SHA, Saidur R, Mahbubul IM, Al-Sulaiman FA. Optical properties of various nanofluids used in solar collector: A review. Renewable and Sustainable Energy Reviews 2017;73:1014–30. https://doi.org/10.1016/j.rser.2017.01.173.
[111] Khullar V, Bhalla V, Tyagi H. Potential Heat Transfer Fluids (Nanofluids) for Direct Volumetric Absorption-Based Solar Thermal Systems. Journal of Thermal Science and Engineering Applications 2017;10. https://doi.org/10.1115/1.4036795.
[112] Mallah AR, Mohd Zubir MN, Alawi OA, Salim Newaz KM, Mohamad Badry AB. Plasmonic nanofluids for high photothermal conversion efficiency in direct absorption solar collectors: Fundamentals and applications. Solar Energy Materials and Solar Cells 2019;201:110084. https://doi.org/10.1016/j.solmat.2019.110084.
[113] Arshad A, Jabbal M, Yan Y, Reay D. A review on graphene based nanofluids: Preparation, characterization and applications. Journal of Molecular Liquids 2019;279:444–84. https://doi.org/10.1016/j.molliq.2019.01.153.
[114] Yılmaz Aydın D, Gürü M. Nanofluids: preparation, stability, properties, and thermal performance in terms of thermo-hydraulic, thermodynamics and thermo-economic analysis. J Therm Anal Calorim 2021. https://doi.org/10.1007/s10973-021-11092-8.

[115] Said Z. Hybrid Nanofluids: Preparation, Characterization and Applications. vol. 1. Elsevier Science; 2022.
[116] Otanicar T, Taylor RA, Phelan PE, Prasher R. Impact of Size and Scattering Mode on the Optimal Solar Absorbing Nanofluid. ASME 2009 3rd International Conference on Energy Sustainability, Volume 1, San Francisco, California, USA: ASMEDC; 2009, p. 791–6. https://doi.org/10.1115/ES2009-90066.
[117] Gorji TB, Ranjbar AA. Thermal and exergy optimization of a nanofluid-based direct absorption solar collector. Renewable Energy 2017;106:274–87. https://doi.org/10.1016/j.renene.2017.01.031.
[118] Chen M, He Y, Zhu J, Wen D. Investigating the collector efficiency of silver nanofluids based direct absorption solar collectors. Applied Energy 2016;181:65–74. https://doi.org/10.1016/j.apenergy.2016.08.054.
[119] Chen M, He Y, Zhu J, Kim DR. Enhancement of photo-thermal conversion using gold nanofluids with different particle sizes. Energy Conversion and Management 2016;112:21–30. https://doi.org/10.1016/j.enconman.2016.01.009.
[120] Amjad M, Raza G, Xin Y, Pervaiz S, Xu J, Du X, et al. Volumetric solar heating and steam generation via gold nanofluids. Applied Energy 2017;206:393–400. https://doi.org/10.1016/j.apenergy.2017.08.144.
[121] Amjad M, Jin H, Du X, Wen D. Experimental photothermal performance of nanofluids under concentrated solar flux. Solar Energy Materials and Solar Cells 2018;182:255–62. https://doi.org/10.1016/j.solmat.2018.03.044.
[122] Chen Z, Chen M, Yan H, Zhou P, Chen X. Enhanced solar thermal conversion performance of plasmonic gold dimer nanofluids. Applied Thermal Engineering 2020;178:115561. https://doi.org/10.1016/j.applthermaleng.2020.115561.
[123] Cai Y, Nan Y, Guo Z. Enhanced absorption of solar energy in a daylighting louver with Ni-water nanofluid. International Journal of Heat and Mass Transfer 2020;158:119921. https://doi.org/10.1016/j.ijheatmasstransfer.2020.119921.
[124] Kundan L, Sharma P. Performance Evaluation of a Nanofluid (CuO-H2O) Based Low Flux Solar Collector. International Journal of Engineering Research 2013:5.
[125] Verma V, Kundan L. Thermal Performance Evaluation of a Direct Absorption Flat Plate Solar Collector (DASC) using Al2O3-H2O Based Nanofluids. IOSR-JMCE 2013;6:29–35. https://doi.org/10.9790/1684-0622935.
[126] Gupta HK, Agrawal GD, Mathur J. An experimental investigation of a low temperature Al2O3-H2O nanofluid based direct absorption solar collector. Solar Energy 2015;118:390–6. https://doi.org/10.1016/j.solener.2015.04.041.
[127] Said Z, Sajid MH, Saidur R, Mahdiraji GA, Rahim NA. Evaluating the Optical Properties of TiO2 Nanofluid for a Direct Absorption Solar Collector. Numerical Heat Transfer, Part A: Applications 2015;67:1010–27. https://doi.org/10.1080/10407782.2014.955344.
[128] Zayats AV, Smolyaninov II, Maradudin AA. Nano-optics of surface plasmon polaritons. Physics Reports 2005;408:131–314. https://doi.org/10.1016/j.physrep.2004.11.001.
[129] Fan X, Zheng W, Singh DJ. Light scattering and surface plasmons on small spherical particles. Light Sci Appl 2014;3:e179–e179. https://doi.org/10.1038/lsa.2014.60.
[130] Won KH, Lee BJ. Effect of light scattering on the performance of a direct absorption solar collector. Front Energy 2018;12:169–77. https://doi.org/10.1007/s11708-018-0527-5.
[131] Mallah AR, Kazi SN, Zubir MNM, Badarudin A. Blended morphologies of plasmonic nanofluids for direct absorption applications. Applied Energy 2018;229:505–21. https://doi.org/10.1016/j.apenergy.2018.07.113.
[132] Lee S, Kim HJ, Kim KH, Jang SP. Extinction coefficient of water-based multi-walled carbon nanotube nanofluids for application in direct-absorption solar collectors. Micro & Nano Letters 2014;9:635–8. https://doi.org/10.1049/mnl.2014.0262.

[133] Lee S-H, Choi TJ, Jang SP. Thermal efficiency comparison: Surface-based solar receivers with conventional fluids and volumetric solar receivers with nanofluids. Energy 2016;115:404–17. https://doi.org/10.1016/j.energy.2016.09.024.
[134] Liu J, Ye Z, Zhang L, Fang X, Zhang Z. A combined numerical and experimental study on graphene/ionic liquid nanofluid based direct absorption solar collector. Solar Energy Materials and Solar Cells 2015;136:177–86. https://doi.org/10.1016/j.solmat.2015.01.013.
[135] Vakili M, Hosseinalipour SM, Delfani S, Khosrojerdi S, Karami M. Experimental investigation of graphene nanoplatelets nanofluid-based volumetric solar collector for domestic hot water systems. Solar Energy 2016;131:119–30. https://doi.org/10.1016/j.solener.2016.02.034.
[136] Karami M, Raisee M, Delfani S, Akhavan Bahabadi MA, Rashidi AM. Sunlight absorbing potential of carbon nanoball water and ethylene glycol-based nanofluids. Opt Spectrosc 2013;115:400–5. https://doi.org/10.1134/S0030400X13090105.
[137] Moradi A, Sani E, Simonetti M, Francini F, Chiavazzo E, Asinari P. Carbon-Nanohorn Based Nanofluids for a Direct Absorption Solar Collector for Civil Application. J Nanosci Nanotechnol 2015;15:3488–95. https://doi.org/10.1166/jnn.2015.9837.
[138] He Q, Wang S, Zeng S, Zheng Z. Experimental investigation on photothermal properties of nanofluids for direct absorption solar thermal energy systems. Energy Conversion and Management 2013;73:150–7. https://doi.org/10.1016/j.enconman.2013.04.019.
[139] Mahian O, Bellos E, Markides CN, Taylor RA, Alagumalai A, Yang L, et al. Recent advances in using nanofluids in renewable energy systems and the environmental implications of their uptake. Nano Energy 2021;86:106069. https://doi.org/10.1016/j.nanoen.2021.106069.
[140] Amin TE, Roghayeh G, Fatemeh R, Fatollah P. Evaluation of Nanoparticle Shape Effect on a Nanofluid Based Flat-Plate Solar Collector Efficiency. Energy Exploration & Exploitation 2015;33:659–76. https://doi.org/10.1260/0144-5987.33.5.659.
[141] Vieira AM, Oliveira NTC, Silva KTPB, Reyna AS. Improving the Performance of Direct Solar Collectors and Stills by Controlling the Morphology and Size of Plasmonic Core–Shell Nanoheaters. J Phys Chem C 2021;125:19653–65. https://doi.org/10.1021/acs.jpcc.1c05952.
[142] Verma SK, Tiwari AK, Tripathi M. An evaluative observation on impact of optical properties of nanofluids in performance of photo-thermal concentrating systems. Solar Energy 2018;176:709–24. https://doi.org/10.1016/j.solener.2018.10.084.
[143] Qin C, Kang K, Lee I, Lee BJ. Optimization of a direct absorption solar collector with blended plasmonic nanofluids. Solar Energy 2017;150:512–20. https://doi.org/10.1016/j.solener.2017.05.007.
[144] Khullar V, Tyagi H, Hordy N, Otanicar TP, Hewakuruppu Y, Modi P, et al. Harvesting solar thermal energy through nanofluid-based volumetric absorption systems. International Journal of Heat and Mass Transfer 2014;77:377–84. https://doi.org/10.1016/j.ijheatmasstransfer.2014.05.023.
[145] Struchalin PG, Yunin VS, Kutsenko KV, Nikolaev OV, Vologzhannikova AA, Shevelyova MP, et al. Performance of a tubular direct absorption solar collector with a carbon-based nanofluid. International Journal of Heat and Mass Transfer 2021;179:121717. https://doi.org/10.1016/j.ijheatmasstransfer.2021.121717.
[146] Bhalla V, Khullar V, Tyagi H. Investigation of factors influencing the performance of nanofluid-based direct absorption solar collector using Taguchi method. J Therm Anal Calorim 2019;135:1493–505. https://doi.org/10.1007/s10973-018-7721-x.
[147] Hooshmand A, Zahmatkesh I, Karami M, Delfani S. Porous foams and nanofluids for thermal performance improvement of a direct absorption solar collector: An experimental study. Environmental Progress & Sustainable Energy 2021;40:e13684. https://doi.org/10.1002/ep.13684.
[148] Siavashi M, Ghasemi K, Yousofvand R, Derakhshan S. Computational analysis of SWCNH nanofluid-based direct absorption solar collector with a metal sheet. Solar Energy 2018;170:252–62. https://doi.org/10.1016/j.solener.2018.05.020.

[149] Tien CL. Thermal Radiation in Packed and Fluidized Beds. Journal of Heat Transfer 1988;110:1230–42. https://doi.org/10.1115/1.3250623.
[150] Karami M, Raisee M, Delfani S. Numerical Investigation of Nanofluid-based Solar Collectors. IOP Conf Ser: Mater Sci Eng 2014;64:012044. https://doi.org/10.1088/1757-899X/64/1/012044.
[151] Wang N, Xu G, Li S, Zhang X. Thermal Properties and Solar Collection Characteristics of Oil-based Nanofluids with Low Graphene Concentration. Energy Procedia 2017;105:194–9. https://doi.org/10.1016/j.egypro.2017.03.301.
[152] Khalil A, Amjad M, Noor F, Hussain A, Nawaz S, Filho EPB, et al. Performance analysis of direct absorption-based parabolic trough solar collector using hybrid nanofluids. J Braz Soc Mech Sci Eng 2020;42:573. https://doi.org/10.1007/s40430-020-02654-2.
[153] Saray JA, Heyhat MM. Modeling of a direct absorption parabolic trough collector based on using nanofluid: 4E assessment and water-energy nexus analysis. Energy 2022;244:123170. https://doi.org/10.1016/j.energy.2022.123170.
[154] Joseph A, Sreekumar S, Thomas S. Energy and exergy analysis of SiO2/Ag-CuO plasmonic nanofluid on direct absorption parabolic solar collector. Renewable Energy 2020;162:1655–64. https://doi.org/10.1016/j.renene.2020.09.139.
[155] Kasaeian A, Daneshazarian R, Pourfayaz F. Comparative study of different nanofluids applied in a trough collector with glass-glass absorber tube. Journal of Molecular Liquids 2017;234:315–23. https://doi.org/10.1016/j.molliq.2017.03.096.
[156] O'Keeffe GJ, Mitchell SL, Myers TG, Cregan V. Modelling the efficiency of a nanofluid-based direct absorption parabolic trough solar collector. Solar Energy 2018;159:44–54. https://doi.org/10.1016/j.solener.2017.10.066.
[157] O'Keeffe GJ, Mitchell SL, Myers TG, Cregan V. Modelling the efficiency of a low-profile nanofluid-based direct absorption parabolic trough solar collector. International Journal of Heat and Mass Transfer 2018;126:613–24. https://doi.org/10.1016/j.ijheatmasstransfer.2018.05.117.
[158] Singh N, Khullar V. On-sun testing of volumetric absorption based concentrating solar collector employing carbon soot nanoparticles laden fluid. Sustainable Energy Technologies and Assessments 2020;42:100868. https://doi.org/10.1016/j.seta.2020.100868.
[159] Khullar V, Tyagi H, Phelan PE, Otanicar TP, Singh H, Taylor RA. Solar Energy Harvesting Using Nanofluids-Based Concentrating Solar Collector. Journal of Nanotechnology in Engineering and Medicine 2012;3:031003. https://doi.org/10.1115/1.4007387.
[160] Li Q, Zheng C, Mesgari S, Hewakuruppu YL, Hjerrild N, Crisostomo F, et al. Experimental investigation of a nanofluid absorber employed in a low-profile, concentrated solar thermal collector. In: Eggleton BJ, Palomba S, editors., Sydney, New South Wales, Australia: 2015, p. 96683P. https://doi.org/10.1117/12.2202513.
[161] Li Q, Zheng C, Mesgari S, Hewkuruppu YL, Hjerrild N, Crisostomo F, et al. Experimental and numerical investigation of volumetric versus surface solar absorbers for a concentrated solar thermal collector. Solar Energy 2016;136:349–64. https://doi.org/10.1016/j.solener.2016.07.015.
[162] Bortolato M, Dugaria S, Agresti F, Barison S, Fedele L, Sani E, et al. Investigation of a single wall carbon nanohorn-based nanofluid in a full-scale direct absorption parabolic trough solar collector. Energy Conversion and Management 2017;150:693–703. https://doi.org/10.1016/j.enconman.2017.08.044.
[163] Dugaria S, Bortolato M, Del Col D. Modelling of a direct absorption solar receiver using carbon based nanofluids under concentrated solar radiation. Renewable Energy 2018;128:495–508. https://doi.org/10.1016/j.renene.2017.06.029.
[164] Kasaeian A, Daneshazarian R, Rezaei R, Pourfayaz F, Kasaeian G. Experimental investigation on the thermal behavior of nanofluid direct absorption in a trough collector. Journal of Cleaner Production 2017;158:276–84. https://doi.org/10.1016/j.jclepro.2017.04.131.

[165] Tafarroj MM, Daneshazarian R, Kasaeian A. CFD modeling and predicting the performance of direct absorption of nanofluids in trough collector. Applied Thermal Engineering 2019;148:256–69. https://doi.org/10.1016/j.applthermaleng.2018.11.020.
[166] Menbari A, Alemrajabi AA, Rezaei A. Experimental investigation of thermal performance for direct absorption solar parabolic trough collector (DASPTC) based on binary nanofluids. Experimental Thermal and Fluid Science 2017;80:218–27. https://doi.org/10.1016/j.expthermflusci.2016.08.023.
[167] Ham J, Shin Y, Cho H. Comparison of thermal performance between a surface and a volumetric absorption solar collector using water and Fe3O4 nanofluid. Energy 2022;239:122282. https://doi.org/10.1016/j.energy.2021.122282.
[168] Xu G, Chen W, Deng S, Zhang X, Zhao S. Performance Evaluation of a Nanofluid-Based Direct Absorption Solar Collector with Parabolic Trough Concentrator. Nanomaterials 2015;5:2131–47. https://doi.org/10.3390/nano5042131.
[169] Chen W, Xu G, Zhao S, Zhang X. Numerical Simulation on the Performance of Nanofluid-Based Direct Absorption Solar Collector With Parabolic Trough Concentrator, Biopolis, Singapore: American Society of Mechanical Engineers; 2016, p. V001T05A012. https://doi.org/10.1115/MNHMT2016-6647.
[170] Heyhat MM, Valizade M, Abdolahzade Sh, Maerefat M. Thermal efficiency enhancement of direct absorption parabolic trough solar collector (DAPTSC) by using nanofluid and metal foam. Energy 2020;192:116662. https://doi.org/10.1016/j.energy.2019.116662.
[171] Menbari A, Alemrajabi AA, Rezaei A. Heat transfer analysis and the effect of CuO/Water nanofluid on direct absorption concentrating solar collector. Applied Thermal Engineering 2016;104:176–83. https://doi.org/10.1016/j.applthermaleng.2016.05.064.
[172] Vishwakarma V, Singhal N, Khullar V, Tyagi H, Taylor RA, Otanicar TP, et al. Space Cooling Using the Concept of Nanofluids-Based Direct Absorption Solar Collectors. Volume 7: Fluids and Heat Transfer, Parts A, B, C, and D, Houston, Texas, USA: American Society of Mechanical Engineers; 2012, p. 2769–77. https://doi.org/10.1115/IMECE2012-87726.
[173] Garg K, Khullar V, Das SK, Tyagi H. Performance evaluation of a brine-recirculation multistage flash desalination system coupled with nanofluid-based direct absorption solar collector. Renewable Energy 2018;122:140–51. https://doi.org/10.1016/j.renene.2018.01.050.
[174] Alagumalai A, Qin C, K E K V, Solomin E, Yang L, Zhang P, et al. Conceptual analysis framework development to understand barriers of nanofluid commercialization. Nano Energy 2022;92:106736. https://doi.org/10.1016/j.nanoen.2021.106736.
[175] Mukherjee S, Mishra PC, Chaudhuri P. Stability of Heat Transfer Nanofluids – A Review. ChemBioEng Reviews 2018;5:312–33. https://doi.org/10.1002/cben.201800008.
[176] Chakraborty S, Panigrahi PK. Stability of nanofluid: A review. Applied Thermal Engineering 2020;174:115259. https://doi.org/10.1016/j.applthermaleng.2020.115259.
[177] Hordy N, Rabilloud D, Meunier J-L, Coulombe S. High temperature and long-term stability of carbon nanotube nanofluids for direct absorption solar thermal collectors. Solar Energy 2014;105:82–90. https://doi.org/10.1016/j.solener.2014.03.013.
[178] Cacua K, Ordoñez F, Zapata C, Herrera B, Pabón E, Buitrago-Sierra R. Surfactant concentration and pH effects on the zeta potential values of alumina nanofluids to inspect stability. Colloids and Surfaces A: Physicochemical and Engineering Aspects 2019;583:123960. https://doi.org/10.1016/j.colsurfa.2019.123960.
[179] Babita, Sharma SK, Gupta SM. Preparation and evaluation of stable nanofluids for heat transfer application: A review. Experimental Thermal and Fluid Science 2016;79:202–12. https://doi.org/10.1016/j.expthermflusci.2016.06.029.
[180] Li X, Zhu D, Wang X. Evaluation on dispersion behavior of the aqueous copper nano-suspensions. Journal of Colloid and Interface Science 2007;310:456–63. https://doi.org/10.1016/j.jcis.2007.02.067.
[181] Wang X-J, Li X-F. Influence of pH on Nanofluids' Viscosity and Thermal Conductivity. Chinese Phys Lett 2009;26:056601. https://doi.org/10.1088/0256-307X/26/5/056601.

[182] Yin Z, Bao F, Tu C, Hua Y, Tian R. Numerical and experimental studies of heat and flow characteristics in a laminar pipe flow of nanofluid. Journal of Experimental Nanoscience 2018;13:82–94. https://doi.org/10.1080/17458080.2017.1413599.
[183] Bepete G, Drummond C, Penicaud A. Aqueous and organic suspensions of exfoliated nanocarbon materials , method for making same and uses thereof. US10 414935, 2019.
[184] Buzea C, Pacheco II, Robbie K. Nanomaterials and nanoparticles: Sources and toxicity. Biointerphases 2007;2:MR17–71. https://doi.org/10.1116/1.2815690.
[185] Fiorito S, Serafino A, Andreola F, Togna A, Togna G. Toxicity and Biocompatibility of Carbon Nanoparticles. J Nanosci Nanotechnol 2006;6:591–9. https://doi.org/10.1166/jnn.2006.125.
[186] Bystrzejewska-Piotrowska G, Golimowski J, Urban PL. Nanoparticles: Their potential toxicity, waste and environmental management. Waste Management 2009;29:2587–95. https://doi.org/10.1016/j.wasman.2009.04.001.
[187] Lam C-W. Pulmonary Toxicity of Single-Wall Carbon Nanotubes in Mice 7 and 90 Days After Intratracheal Instillation. Toxicological Sciences 2003;77:126–34. https://doi.org/10.1093/toxsci/kfg243.
[188] Dreher KL. Health and Environmental Impact of Nanotechnology: Toxicological Assessment of Manufactured Nanoparticles. Toxicological Sciences 2003;77:3–5. https://doi.org/10.1093/toxsci/kfh041.
[189] Schrand AM, Rahman MF, Hussain SM, Schlager JJ, Smith DA, Syed AF. Metal-based nanoparticles and their toxicity assessment. WIREs Nanomed Nanobiotechnol 2010;2:544–68. https://doi.org/10.1002/wnan.103.
[190] Elsaid K, Olabi AG, Wilberforce T, Abdelkareem MA, Sayed ET. Environmental impacts of nanofluids: A review. Science of The Total Environment 2021;763:144202. https://doi.org/10.1016/j.scitotenv.2020.144202.
[191] Otanicar TP, Golden JS. Comparative Environmental and Economic Analysis of Conventional and Nanofluid Solar Hot Water Technologies. Environ Sci Technol 2009;43:6082–7. https://doi.org/10.1021/es900031j.
[192] Gupta HK, Agrawal GD, Mathur J. Assessment of energy and economic advantages by proposing nanofluid based direct absorption in solar collectors for India. International Conference on Recent Advances and Innovations in Engineering (ICRAIE-2014), Jaipur, India: IEEE; 2014, p. 1–8. https://doi.org/10.1109/ICRAIE.2014.6909133.
[193] Part F, Zecha G, Causon T, Sinner E-K, Huber-Humer M. Current limitations and challenges in nanowaste detection, characterisation and monitoring. Waste Management 2015;43:407–20. https://doi.org/10.1016/j.wasman.2015.05.035.
[194] Younis SA, El-Fawal EM, Serp P. Nano-wastes and the Environment: Potential Challenges and Opportunities of Nano-waste Management Paradigm for Greener Nanotechnologies. In: Hussain CM, editor. Handbook of Environmental Materials Management, Cham: Springer International Publishing; 2018, p. 1–72. https://doi.org/10.1007/978-3-319-58538-3_53-1.
[195] Omrani AN, Esmaeilzadeh E, Jafari M, Behzadmehr A. Effects of multi walled carbon nanotubes shape and size on thermal conductivity and viscosity of nanofluids. Diamond and Related Materials 2019;93:96–104. https://doi.org/10.1016/j.diamond.2019.02.002.
[196] Chiam HW, Azmi WH, Usri NA, Mamat R, Adam NM. Thermal conductivity and viscosity of Al2O3 nanofluids for different based ratio of water and ethylene glycol mixture. Experimental Thermal and Fluid Science 2017;81:420–9. https://doi.org/10.1016/j.expthermflusci.2016.09.013.
[197] Celata GP, D'Annibale F, Mariani A, Sau S, Serra E, Bubbico R, et al. Experimental results of nanofluids flow effects on metal surfaces. Chemical Engineering Research and Design 2014;92:1616–28. https://doi.org/10.1016/j.cherd.2013.12.003.
[198] Fotowat S, Askar S, Ismail M, Fartaj A. A study on corrosion effects of a water based nanofluid for enhanced thermal energy applications. Sustainable Energy Technologies and Assessments 2017;24:39–44. https://doi.org/10.1016/j.seta.2017.02.001.

[199] Rashmi W, Ismail AF, Khalid M, Anuar A, Yusaf T. Investigating corrosion effects and heat transfer enhancement in smaller size radiators using CNT-nanofluids. J Mater Sci 2014;49:4544–51. https://doi.org/10.1007/s10853-014-8154-y.
[200] Srinivas V, Moorthy ChVKNSN, Dedeepya V, Manikanta PV, Satish V. Nanofluids with CNTs for automotive applications. Heat Mass Transfer 2016;52:701–12. https://doi.org/10.1007/s00231-015-1588-1.
[201] Wciślik S. A simple economic and heat transfer analysis of the nanoparticles use. Chem Pap 2017;71:2395–401. https://doi.org/10.1007/s11696-017-0234-4.
[202] Alirezaie A, Hajmohammad MH, Alipour A, salari M. Do nanofluids affect the future of heat transfer?"A benchmark study on the efficiency of nanofluids." Energy 2018;157:979–89. https://doi.org/10.1016/j.energy.2018.05.060.
[203] Otanicar TP, Chowdhury I, Prasher R, Phelan PE. Band-Gap Tuned Direct Absorption for a Hybrid Concentrating Solar Photovoltaic/Thermal System. Journal of Solar Energy Engineering 2011;133:041014. https://doi.org/10.1115/1.4004708.
[204] Zhao J, Song Y, Lam W-H, Liu W, Liu Y, Zhang Y, et al. Solar radiation transfer and performance analysis of an optimum photovoltaic/thermal system. Energy Conversion and Management 2011;52:1343–53. https://doi.org/10.1016/j.enconman.2010.09.032.
[205] Cui Y, Zhu Q. Study of Photovoltaic/Thermal Systems with MgO-Water Nanofluids Flowing over Silicon Solar Cells. 2012 Asia-Pacific Power and Energy Engineering Conference, Shanghai, China: IEEE; 2012, p. 1–4. https://doi.org/10.1109/APPEEC.2012.6307203.
[206] Taylor RA, Otanicar T, Rosengarten G. Nanofluid-based optical filter optimization for PV/T systems. Light Sci Appl 2012;1:e34–e34. https://doi.org/10.1038/lsa.2012.34.
[207] Otanicar TP, Taylor RA, Telang C. Photovoltaic/thermal system performance utilizing thin film and nanoparticle dispersion based optical filters. Journal of Renewable and Sustainable Energy 2013;5:033124. https://doi.org/10.1063/1.4811095.
[208] Taylor RA, Otanicar TP, Herukerrupu Y, Bremond F, Rosengarten G, Hawkes ER, et al. Feasibility of nanofluid-based optical filters. Appl Opt 2013;52:1413. https://doi.org/10.1364/AO.52.001413.
[209] DeJarnette D, Otanicar T, Brekke N, Hari P, Roberts K, Saunders AE, et al. Plasmonic nanoparticle based spectral fluid filters for concentrating PV/T collectors. In: Plesniak AP, Pfefferkorn C, editors., San Diego, California, United States: 2014, p. 917509. https://doi.org/10.1117/12.2064680.
[210] Saroha S, Mittal T, Modi PJ, Bhalla V, Khullar V, Tyagi H, et al. Theoretical Analysis and Testing of Nanofluids-Based Solar Photovoltaic/Thermal Hybrid Collector. Journal of Heat Transfer 2015;137:091015. https://doi.org/10.1115/1.4030228.
[211] An W, Wu J, Zhu T, Zhu Q. Experimental investigation of a concentrating PV/T collector with Cu9S5 nanofluid spectral splitting filter. Applied Energy 2016;184:197–206. https://doi.org/10.1016/j.apenergy.2016.10.004.
[212] An W, Zhang J, Zhu T, Gao N. Investigation on a spectral splitting photovoltaic/thermal hybrid system based on polypyrrole nanofluid: Preliminary test. Renewable Energy 2016;86:633–42. https://doi.org/10.1016/j.renene.2015.08.080.
[213] Hjerrild NE, Mesgari S, Crisostomo F, Scott JA, Amal R, Taylor RA. Hybrid PV/T enhancement using selectively absorbing Ag–SiO 2 /carbon nanofluids. Solar Energy Materials and Solar Cells 2016;147:281–7. https://doi.org/10.1016/j.solmat.2015.12.010.
[214] Otanicar TP, DeJarnette D, Hewakuruppu Y, Taylor RA. Filtering light with nanoparticles: a review of optically selective particles and applications. Adv Opt Photon 2016;8:541. https://doi.org/10.1364/AOP.8.000541.
[215] An W, Li J, Ni J, Taylor RA, Zhu T. Analysis of a temperature dependent optical window for nanofluid-based spectral splitting in PV/T power generation applications. Energy Conversion and Management 2017;151:23–31. https://doi.org/10.1016/j.enconman.2017.08.080.

[216] Crisostomo F, Hjerrild N, Mesgari S, Li Q, Taylor RA. A hybrid PV/T collector using spectrally selective absorbing nanofluids. Applied Energy 2017;193:1–14. https://doi.org/10.1016/j.apenergy.2017.02.028.
[217] Widyolar BK, Abdelhamid M, Jiang L, Winston R, Yablonovitch E, Scranton G, et al. Design, simulation and experimental characterization of a novel parabolic trough hybrid solar photovoltaic/thermal (PV/T) collector. Renewable Energy 2017;101:1379–89. https://doi.org/10.1016/j.renene.2016.10.014.
[218] Yazdanifard F, Ameri M, Ebrahimnia-Bajestan E. Performance of nanofluid-based photovoltaic/thermal systems: A review. Renewable and Sustainable Energy Reviews 2017;76:323–52. https://doi.org/10.1016/j.rser.2017.03.025.
[219] Brekke N, Dale J, DeJarnette D, Hari P, Orosz M, Roberts K, et al. Detailed performance model of a hybrid photovoltaic/thermal system utilizing selective spectral nanofluid absorption. Renewable Energy 2018;123:683–93. https://doi.org/10.1016/j.renene.2018.01.025.
[220] Ni J, Li J, An W, Zhu T. Performance analysis of nanofluid-based spectral splitting PV/T system in combined heating and power application. Applied Thermal Engineering 2018;129:1160–70. https://doi.org/10.1016/j.applthermaleng.2017.10.119.
[221] Otanicar T, Dale J, Orosz M, Brekke N, DeJarnette D, Tunkara E, et al. Experimental evaluation of a prototype hybrid CPV/T system utilizing a nanoparticle fluid absorber at elevated temperatures. Applied Energy 2018;228:1531–9. https://doi.org/10.1016/j.apenergy.2018.07.055.
[222] Hjerrild NE, Crisostomo F, Chin RL, Scott JA, Amal R, Taylor RA. Experimental Results for Tailored Spectrum Splitting Metallic Nanofluids for c-Si, GaAs, and Ge Solar Cells. IEEE J Photovoltaics 2019;9:385–90. https://doi.org/10.1109/JPHOTOV.2018.2883626.
[223] Li H, He Y, Wang C, Wang X, Hu Y. Tunable thermal and electricity generation enabled by spectrally selective absorption nanoparticles for photovoltaic/thermal applications. Applied Energy 2019;236:117–26. https://doi.org/10.1016/j.apenergy.2018.11.085.
[224] Goel N, Taylor RA, Otanicar T. A review of nanofluid-based direct absorption solar collectors: Design considerations and experiments with hybrid PV/Thermal and direct steam generation collectors. Renewable Energy 2020;145:903–13. https://doi.org/10.1016/j.renene.2019.06.097.
[225] Hemmat Esfe M, Kamyab MH, Valadkhani M. Application of nanofluids and fluids in photovoltaic thermal system: An updated review. Solar Energy 2020;199:796–818. https://doi.org/10.1016/j.solener.2020.01.015.
[226] Cui Y, Zhu J, Zoras S, Zhang J. Comprehensive review of the recent advances in PV/T system with loop-pipe configuration and nanofluid. Renewable and Sustainable Energy Reviews 2021;135:110254. https://doi.org/10.1016/j.rser.2020.110254.